SPEED CONTROL OF BLDC MOTOR DRIVE USING SVPWM INVERTER

A thesis submitted in partial fulfilment of the requirements for the degree

Of

Master of Technology

in

Electrical Engineering
(Specialization Industrial Electronics)

by

Mendi Balaji

(Roll.no:213ee5339)

Department of Electrical Engineering
National Institute of Technology Rourkela
Rourkela, Odisha-769008
2015

SPEED CONTROL OF BLDC MOTOR DRIVE USING SVPWM INVERTER

A thesis submitted in partial fulfilment of the requirements for the degree

of

Master of Technology

in

Electrical Engineering
(Specialization Industrial Electronics)

By

Mendi Balaji

Under the Guidance of

Dr. Susovon Samanta

Department of Electrical Engineering
National Institute of Technology Rourkela
Rourkela, Odisha-769008
2015

National Institute of Technology

Rourkela

CERTIFICATE

This is to certify that the thesis entitled, "**Speed Control of SVPWM Inverter fed BLDC Motor Drive**" submitted by **Mendi Balaji** in partial fulfilment of the requirements for the award of MASTER of Technology Degree in Electrical Engineering with specialization in "**Industrial Electronics**" at the National Institute of Technology, Rourkela (Deemed University) is an authentic work carried out by him/her under my/our supervision and guidance. To the best of my knowledge, the matter embodied in the thesis has not been submitted to any other University/ Institute for the award of any degree or diploma.

Date:

Dr. S. Samanta
Dept. of Electrical Engg.
National Institute of Technology
Rourkela - 769008

Acknowledgment

First and Foremost, I would like to express my sincere gratitude towards my supervisor **Dr. Susovon Samanta** for his advice during my project work. He has constantly encouraged me to remain focused on achieving my goal. His observations and comments helped me to establish the overall direction of the research and to move forward with investigation in depth. He has helped me greatly and been a source of knowledge. I extend my thanks to our HOD, **Prof. A.K Panda** and to all the professors of the department for their support and encouragement.

I am really thankful to my batch mates who helped me during my course work and also in writing the thesis. My sincere thanks to everyone who has provided me with kind words, a welcome ear, new ideas, useful criticism, or their invaluable time, I am truly indebted.

I must acknowledge the academic resources that I have got from NIT Rourkela. I would like to thank administrative and technical staff members of the Department who have been kind enough to advise and help in their respective roles.

Last, but not the least, I would like to acknowledge the love, support and motivation I received from my parents and therefore I dedicate this thesis to my family.

Mendi Balaji

213EE5339

ABSTRACT

BLDC motors find applications in Automotive (especially) electric vehicle (EV)), appliance and industries because it does not require mechanical commutator used in traditional motors, replacing it with an electronic commutator that commutator improves the reliability and durability of the motor. Three phase voltage source inverter feeds power to the BLDC motor. It is operated by energizing two of its three phase windings at a time. This makes efficient use of windings and develops higher motor torque. The energization of the stator windings are dependent on the position of the rotor. Hall sensors are used for determining the position of the rotor. Based on the position of the rotor the switching devices in the inverter are commutated for every 60^0 degrees. The inverter gives desirable voltage and output frequency by controlling the switching times on or off using PWM techniques. There are various PWM techniques, among these sinusoidal PWM method and space vector PWM methods are mostly used today. SVPWM inverter gives better dc-bus voltage utilization, lower switching losses and better harmonic performance in comparison to the carrier based sine PWM inverter. PI controller is used for the speed control of the BLDC motor which leads to improve the behaviour of the motor. The SVPWM technique and speed control of the BLDC motor is simulated using the MATLAB Software package.

Contents

List of figures

List of tables

List of symbols

k_p = Proportional controller gain

k_i = Integral controller gain

k_d = Derivative controller gain

R_s = Stator resistance per phase

L = Inductance per phase

ω_m = Motor speed

ω_{ref} = Reference motor speed

T_e = electromagnetic torque

E_a, E_b, E_c = Back emf of stator phase winding aa'

$i_a, \mathrm{i}_b, \mathrm{i}_c$ = Phase current of stator winding aa'

H_A, H_B, H_C = Hall sensor signals

V_a, V_b, V_c = Three phase voltages

V_{ref} = Reference voltage

V_{dc} = Inverter input voltage

T_z = Sampling time

f_s = Switching frequency

f = Inverter frequency

θ = Rotor position

M = Mutual inductance between any two windings

J = Moment of inertia

T_l = Load torque

B = Friction constant

λ_m = Peak flux linkage of the permanent magnet rotor

Chapter-1

Introduction

1.1 Overview

Brushless DC motor is a permanent magnet synchronous motor which is powered by dc-voltage through the inverter that produces the ac electric signal to drive the motor. The torque-speed characteristics of the BLDC motor are similar to the BRUSHED DC motor, that's why the name BLDC came. The commutation is done in BLDCM is electronically instead of brushes. It is easily controlled through the rotor position sensors and performs well especially in speed/torque. With these advantages, the motor will spread to more applications. The applications of BLDCM are increased and its competing with the induction motors and dc motors. The output voltage and output frequency of the inverter are dependent on the switching state of the inverter. The controlling of the inverter switches is done by using various PWM techniques, among these sine PWM and space vector PWM methods are mostly used today due to many advantages. SVPWM is easy to digitalize and having lower switching losses and consists lesser harmonics and the better utilization of the dc-bus voltage in comparison with SPWM method. With these advantages the use of SVPWM microcontroller become most important PWM methods for inverters. The speed of the BLDC motor is controlled using SVPWM inverter have many advantages such as the pulsating torque will be minimised, the THD of the current and voltage waveforms of the motor are reduced, and it utilization of dc-bus voltage will be better.

1.2 Literature review

Permanent magnet Brushless direct current (PMBLDC) motors have more advantages than any other motors like induction motors, dc motors due to compact size, higher efficiency, noiseless operation , higher dynamic response, longer life, and electronic commutation [1]. BLDC motor has trapezoidal back EMF and phase current is rectangular waveforms which gives zero torque ripple [2]. The BLDC motor is controlled using three phase voltage source inverter. This VSI feeds power to the motor. Inverter controls the output voltage and the frequency by varying ON/OFF of the switching devices. Each switch is operating 120 degrees [8]. In BLDC motor only two phase windings are energized at a time and the third phase kept opened. These two phase windings are connected to the two switching devices of the inverter. Each phase is conducting 120 degrees the commutation happens for every 60 degrees. The

commutation of the BLDC motor is depends on the rotor position of the motor [3]. The rotor position can be determined by placing hall sensors on the stator of the motor at each phase which are displaced by 120 degrees. Pulsating torque and its minimization techniques are studied [3]. The speed control of BLDC motor with SVPWM inverter gives better utilization of dc link input voltage, lesser switching losses, and lesser total harmonic distortion than the other PWM techniques [4]. SVPWM inverter can be digitalized easily. The concept of space vector is derived from the rotating magnetic field theory of induction motor. By using Clark's transformation three phase voltages are converted to two phase voltages for easy analysis and computations [9]. The implementation of SVPWM inverter is done using MATLAB Simulink software and results are compared with SPWM inverter [4]. Therefore SVPWM inverter control is more suitable to the BLDC motor than SPWM inverter [12, 13]. Various types of topologies of PMBLDC motor with voltage source inverter (VSI) are studied [5]. The mathematical modelling of BLDC motor analysis has been studied [6, 7]. The transfer function of BLDC motor and DC motor are same and the difference is only mechanical time constant and electrical time constant values will be varied. By using this transfer function the speed controller of the BLDC motor is designed [10]. The PID controller tuning design can be done in many ways, which are Ziegler Nicholas tuning method, lead-lag compensator design method, and Routh Hurwitz array method etc. For better accuracy the Kp, Ki, and Kd values are designed by using Ziegler Nicholas method [11]. The implementation of SVPWM inverter with BLDC motor is done in MATLAB Simulink software and the results are compared with the basic BLDC motor control with the commutation sequence of 120 degree inverter.

1.3 Motivation

The usage of BLDC motors are increased in the industries, automobiles, due to better torque speed characteristics, compact size, higher efficiency, wide speed range and longer operational life. In permanent magnet synchronous motors (PMSM) the stator winding back emf is sinusoidal, but in BLDC motor the shape of the back emf is trapezoidal waveform, so that copper saving is more in BLDC motor than the PMSM. The phase current in the BLDC motor is rectangular so that it gives the zero ripple torque ideally. The speed control of the motor is done by using three phase voltage source inverter (VSI) which feeds power to the motor. There are so many pulse width modulation techniques to give better inverter output voltage and the frequency, out of which SPWM and the SVPWM techniques are desirable. The SVPWM technique have many advantages than the SPWM method. In SVPWM only one switch is

operating at a time. So switching losses are less. SVPWM inverter provides 15.5% dc-link input voltage to the BLDC motor and total harmonic distortion is lesser. And also the switching frequency of the inverter is less in the SVPWM inverter so that the efficiency of the inverter is more. SVPWM inverter can be digitalized easily and also the implementation in micro controller is easier. Therefore the SVPWM inverter is more suitable to the speed control of BLDC motor.

1.4 Objectives

The objectives of the speed control of the BLDC motor with SVPWM inverter for electric vehicle are

- To implement the SVPWM inverter in MATLAB Simulink software.
- To design the speed controller of the BLDC motor.
- To implement the BLDC motor with 120 degree switch on mode inverter using MATLAB Simulink software.
- To implement the BLDC motor with SVPWM inverter using MATLAB Simulink software.

1.5 Work done of the speed control of the BLDC motor with SVPWM inverter

The block diagram of the speed control of the BLDC motor with SVPWM inverter is shown below. The BLDC motor is energized by the three phase VSI inverter. The DC voltage Vdc applied to the inverter. The rotor position of the BLDC motor is sensed by hall sensors which are placed on the three phase stator winding coils, and the hall sensors are displaced by 60 degrees apart. The commutation sequence is determined by using rotor position. The actual speed of the motor is sensed and it is compared with the reference speed so that the error is taken as input to the speed controller. Here the speed controller is PID controller which gives the desired output by choosing Kp, Ki, and Kd values. The best PID controller tuning technique is Zigler-Nicholos tuning method which gives the suitable Kp, Ki, and Kd values. The output of the speed controller is gives the peak voltage.

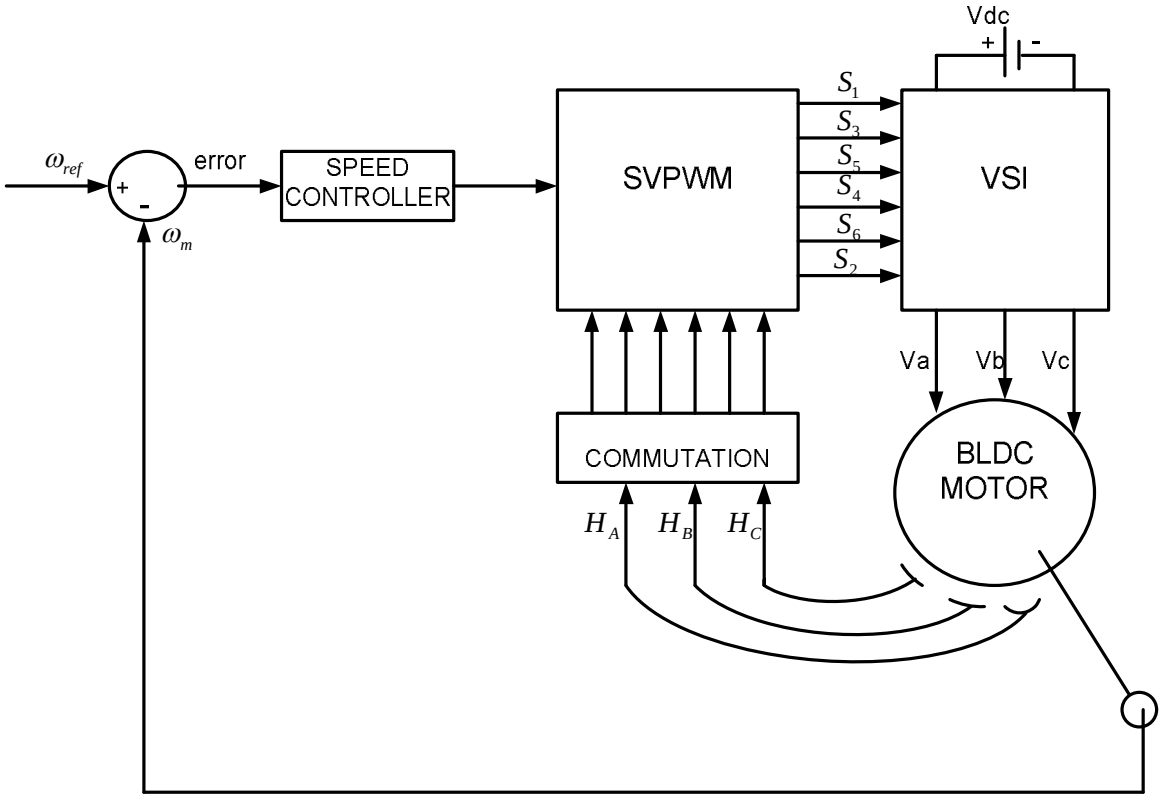

FIG.1: BLOCK DIAGRAM OF THE SPEED CONTROL OF THE BLDC MOTOR WITH SVPWM INVERTER

The three phase voltages V_a^*, V_b^* and V_c^* are generated by taking the inputs which are inverter output frequency, clock time and the peak voltage which comes from the speed controller. By using the Clark's transformation method the three phase voltages V_a^*, V_b^* and V_c^* are converted to the two phase voltages V_α and V_β in the stationary reference frame. The two phase voltages V_α and V_β gives the reference voltage Vref and the angle. By using this angle the sector number N is determined. These are the inputs Vref, sector number N, the switching frequency fs and the sampling time Tz which generates the space vector PWM pulses. These SVPWM pulses are multiplied with the commutation sequence so that each switching device conducts 120 degrees and the commutation occurs at every 60 degrees. These multiplied PWM pulses are given to the three VSI inverter. In this way the speed control of the BLDC motor is done.

1.6 Organization of the Thesis

Chapter-1: the first chapter describes the brief introduction, literature review, motivation, objective and the work done of the speed control of the BLDC motor with SVPWM inverter is described.

Chapter-2: the second chapter describes the principle and implementation of the SVPWM inverter.

Chapter-3: the third chapter describes the BLDC motor principle, the mathematical modelling and the pulsating torque in the BLDC motor.

Chapter-4: the fourth chapter describes the controller design of the BLDC motor.

Chapter-5: the fifth chapter describes the simulation results and the discussions.

Chapter-6: the sixth chapter describes the conclusion and the future work.

Chapter-2

Space vector pulse width modulation method (SVPWM)

2.1. Introduction

Space vector pulse width modulation method is best among all the PWM techniques for drive applications and the three phase voltage source inverters (VSI). Compared to sinusoidal pulse width modulation Method (SPWM), SVPWM has many advantages, which are less switching losses, less total harmonic distortion, it is easy to digitalize and better utilization of dc-bus voltage. The performance of the SVPWM inverter is based on the following criteria: switching losses of the inverter, total harmonic distortion (THD) and maximum output voltage. Originally the SVPWM method is developed as a vector approach to pulse width modulation (PWM) for three phase inverters. In SVPWM inverter the reference wave is revolving reference voltage vector and the carrier signal is high frequency triangular or saw tooth waveform. The intersection of these two will give the gate pulses to inverter to control the voltage and frequency of the inverter.

2.2 Features of SVPWM

The SVPWM is better than the other PWM methods due to the following features.

- It has the wide linear modulation range including with PWM third harmonic injection automatically.
- It has lesser switching losses because only one switch is operating at a time in the SVPWM inverter.
- It gives 15.5% more utilization of DC-Link voltage than the conventional PWM methods.
- It has higher efficiency.
- It gives output phase voltage is $\frac{V_{dc}}{\sqrt{3}}$ and output line voltage is V_{dc},but in SPWM the output phase voltage is $\frac{V_{dc}}{2}$, output line voltage is $\frac{\sqrt{3}V_{dc}}{2}$,therefore SVPWM gives more output phase and line voltages than the SPWM inverter.
- It is a digital modulating technique.

2.3 Concept of space vector

The space vector concept is derived from rotating magnetic field theory of three phase induction motor which is used for modulating the inverter output voltage. In this method three phase voltages are transformed to two phase voltages either in stationary reference frame or synchronous rotating reference frame. Using this two phase voltage reference components the inverter output can be modulated.

Let us take the three phase balanced voltages as shown below,

$$V_{as} = V_m \sin \omega t \tag{2.1}$$

$$V_{bs} = V_m \sin\left(\omega t - \frac{2\pi}{3}\right) \tag{2.2}$$

$$V_{cs} = V_m \sin\left(\omega t + \frac{2\pi}{3}\right) \tag{2.3}$$

If we apply these three phase balanced voltages to the three phase induction motor, it produces rotating flux vector in the air gap of the induction machine rotating with a velocity of ω. This rotating flux vector magnitude and angle can be calculated using the Clark's transformation method in stationary reference frame as shown below.

$$\vec{V}_{ref} = \vec{V}_{\alpha} + j\vec{V}_{\beta} = \frac{2}{3}\left(V_a + V_b e^{j\frac{2\pi}{3}} + V_c e^{j\frac{4\pi}{3}}\right) \tag{2.4}$$

Where $\left|V_{ref}\right| = \sqrt{\left(V_{\alpha}^2 + V_{\beta}^2\right)}$ and $\alpha = \tan^{-1}\frac{V_{\beta}}{V_{\alpha}}$ (2.5)

The above equation is separated into real and imaginary parts which are

$$V_{\alpha} = \frac{2}{3}\left(V_a \cos 0 + V_b \cos\frac{2\pi}{3} + V_c \cos\frac{4\pi}{3}\right) \tag{2.6}$$

$$V_{\beta} = \frac{2}{3}\left(V_a \sin 0 + V_b \sin\frac{2\pi}{3} + V_c \sin\frac{4\pi}{3}\right) \tag{2.7}$$

The above equations can be represented in matrix form as shown below

$$\begin{bmatrix} V_\alpha \\ V_\beta \end{bmatrix} = \begin{bmatrix} 1 & \frac{-1}{2} & \frac{-1}{2} \\ 0 & \frac{\sqrt{3}}{2} & \frac{-\sqrt{3}}{2} \end{bmatrix} \begin{bmatrix} V_{as} \\ V_{bs} \\ V_{cs} \end{bmatrix} \quad (2.8)$$

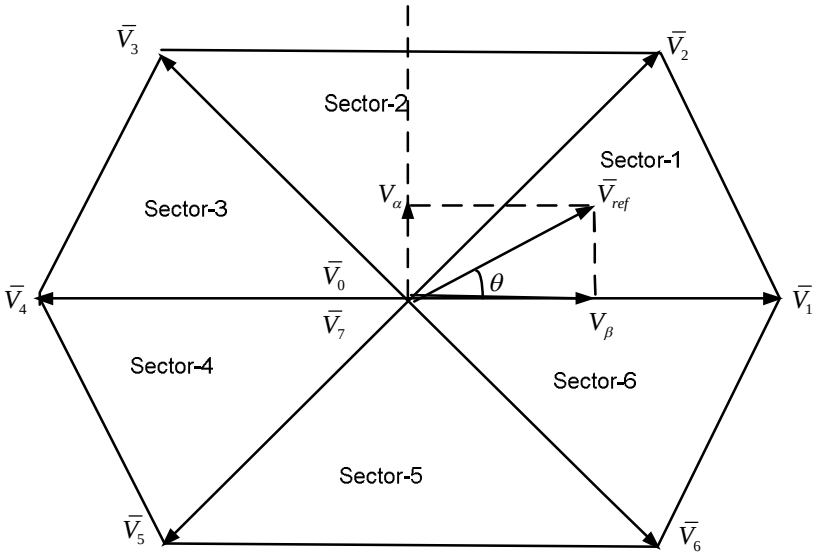

Fig2.1: Representation of rotating vector in complex plane

2.4. Principle of Space Vector PWM

The three phase voltage source inverter (VSI) with BLDC motor load is shown in figure 2. It has three legs that have two switching devices and those are complimenting each other. i.e. only one switch is operating at a time. Therefore the output voltage of the inverter is determined by the ON/OFF of the three switching devices (S1, S3, and S5).

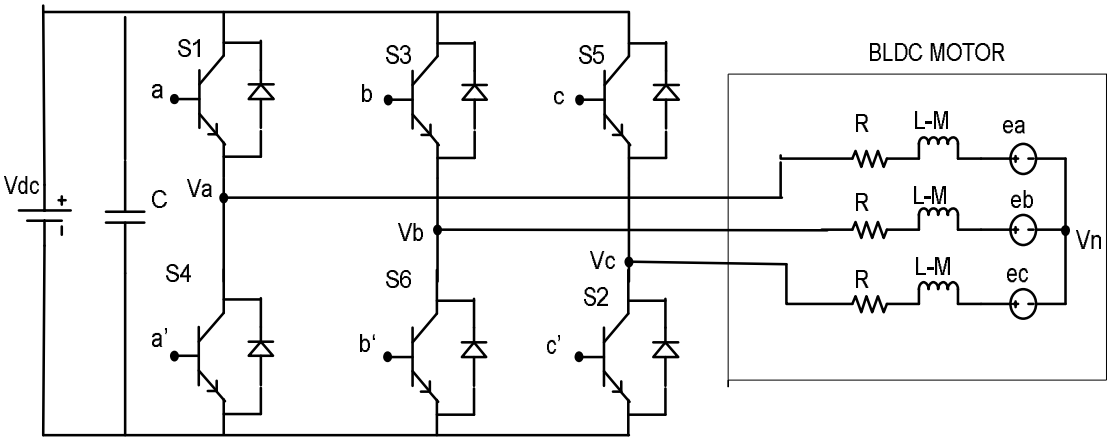

Fig2.2. Three phase VSI with BLDC motor

The output voltage is controlled by the switching variables a, b, c, a', b' and c'. If the upper switch is ON then the switching variable a, b, or c is 1, then the corresponding switching device is OFF, then the switching variable a', b', or c' is 0. The following matrix gives the relation between switching variable and the output phase voltages and output line voltages.

$$\begin{bmatrix} V_{an} \\ V_{bn} \\ V_{cn} \end{bmatrix} = V_{dc} \begin{bmatrix} 1 & -1 & 0 \\ 0 & 1 & -1 \\ -1 & 0 & 1 \end{bmatrix} \begin{bmatrix} a \\ b \\ c \end{bmatrix} \tag{2.9}$$

$$\begin{bmatrix} V_{ab} \\ V_{bc} \\ V_{ca} \end{bmatrix} = \frac{V_{dc}}{3} \begin{bmatrix} 2 & -1 & -1 \\ -1 & 2 & -1 \\ -1 & -1 & 2 \end{bmatrix} \begin{bmatrix} a \\ b \\ c \end{bmatrix} \tag{2.10}$$

Inverter has eight possible switching states out of which six switching states gives six active voltage vectors and two switching states gives two null vectors. Based on the equations (2.4), (2.9) and (2.10) inverter output phase voltages, output line voltages and voltage vectors are determined which are in the tabular form-1.

Voltage vectors $(\times V_{dc})$	Switching vectors			Output phase voltages $(\times V_{dc})$			Output line voltages $(\times V_{dc})$		
	a	b	C	Van	Vbn	Vcn	Vab	Vbc	Vca
$\bar{V}_0 = 0$	0	0	0	0	0	0	0	0	0
$\bar{V}_1 = \frac{2}{3} e^{j\frac{\pi}{3}}$	0	0	1	$\frac{2}{3}$	$\frac{-1}{3}$	$\frac{-1}{3}$	1	0	-1
$\bar{V}_2 = \frac{2}{3} e^{j\frac{2\pi}{3}}$	0	1	0	$\frac{1}{3}$	$\frac{1}{3}$	$\frac{-2}{3}$	0	1	-1
$\bar{V}_3 = \frac{2}{3} e^{j\pi}$	0	1	1	$\frac{-1}{3}$	$\frac{2}{3}$	$\frac{-1}{3}$	-1	1	0
$\bar{V}_4 = \frac{2}{3} e^{j\frac{4\pi}{3}}$	1	0	0	$\frac{-2}{3}$	$\frac{1}{3}$	$\frac{1}{3}$	-1	0	1

$\bar{V}_5 = \frac{2}{3}e^{j\frac{5\pi}{3}}$	1	0	1	$\frac{-1}{3}$	$\frac{-1}{3}$	$\frac{2}{3}$	0	-1	1
$\bar{V}_6 = \frac{2}{3}e^{j2\pi}$	1	1	0	$\frac{1}{3}$	$\frac{-2}{3}$	$\frac{1}{3}$	1	-1	0
$\bar{V}_7 = 0$	1	1	1	0	0	0	0	0	0

Table-2.1: inverter output voltages switching states and corresponding voltage vectors

2.5. Implementation of Space Vector PWM

SVPWM can be implemented in three steps which are

i. Calculation of, V_d V_q and α .

ii. Calculation of T_1, T_2 and T_0 .

iii. Calculation of switching time of each switching device (S1 TO S6).

2.6 Calculation of V_d V_q and α .

Using Clark's transformation three phase voltages are transformed to two phase voltages in $\alpha\beta$ stationary reference frame that is shown in figure.

$$V_d = \left(V_a \cos 0 + V_b \cos\frac{2\pi}{3} + V_c \cos\frac{4\pi}{3} \right)$$

$$= V_a - \frac{1}{2}V_b - \frac{1}{2}V_c \qquad (2.11)$$

$$V_q = \left(V_a \sin 0 + V_b \sin\frac{2\pi}{3} + V_c \sin\frac{4\pi}{3} \right)$$

$$= \frac{\sqrt{3}}{2}V_b - \frac{\sqrt{3}}{2}V_c \qquad (2.12)$$

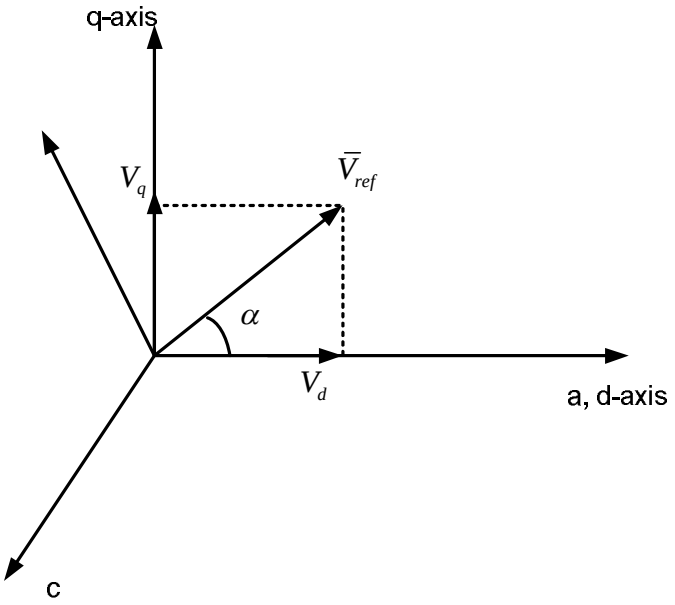

Fig2.3: Reference vector in the two and three dimensional plane

$$\begin{bmatrix} V_d \\ V_q \end{bmatrix} = \begin{bmatrix} 1 & \frac{-1}{2} & \frac{-1}{2} \\ 0 & \frac{\sqrt{3}}{2} & \frac{-\sqrt{3}}{2} \end{bmatrix} \begin{bmatrix} V_{an} \\ V_{bn} \\ V_{cn} \end{bmatrix} \tag{2.13}$$

Where $\left|V_{ref}\right| = \sqrt{\left(V_d^2 + V_q^2\right)}$ and $\alpha = \tan^{-1}\frac{V_q}{V_d}$ (2.14)

2.7 Calculation of T_1, T_2 and T_0.

i. Calculation of $T_1, T_2 and T_0$ in sector-1:

For generating a voltage vector Vref in sector-1 at a sampling T_z time of , it requires two active voltage vectors and two null vectors. Let $\overline{V}_1$ is the active voltage vector applied at fraction of time $\frac{T_1}{T_z}$ interval, and $\overline{V}_2$ is the active voltage vector applied at time $\frac{T_2}{T_z}$, and $\overline{V}_0$ and $\overline{V}_7$ are two null vectors which are applied at a time intervals of $\frac{T_0}{T_z}$ and $\frac{T_7}{T_z}$ respectively. Below figure represents the generation of Vref vector in sector-1.

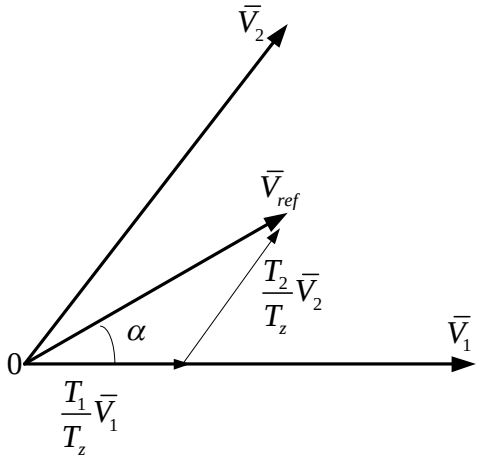

Fig 2.4. Calculation $\bar{V}_{ref}$ in sector-1

Using volt-sec balance equation $\bar{V}_{ref}$ calculated as follows

$$\frac{1}{T_z}\int_0^{T_z}\bar{v}_{ref}\,dt = \frac{1}{T}\left[\int_0^{T_0}\bar{v}_0 dt + \int_0^{T_1}\bar{v}_1 dt + \int_0^{T_2}\bar{v}_2 dt + \int_0^{T_7}\bar{v}_7 dt\right] \tag{2.15}$$

$$T_z\bar{V}_{ref} = T_1\bar{V}_1 + T_2\bar{V}_2 \tag{2.16}$$

$$\bar{V}_{ref} = \frac{T_1}{T_z}\bar{V}_1 + \frac{T_2}{T_z}\bar{V}_2 \tag{2.17}$$

$$T_z = T_1 + T_2 + T_n$$

Where $T_n = T_0 + T_7$, and $|V_1| = |V_2| = |V_3| = |V_4| = |V_5| = |V_6| = |V_0| = |V_7| = \frac{2}{3}V_{dc}$, and $0 \le \alpha \le \frac{\pi}{3}$

$$T_z\left|V_{ref}\right|\begin{bmatrix}\cos\alpha\\ \sin\alpha\end{bmatrix} = T_1\frac{2}{3}V_{dc}\begin{bmatrix}1\\0\end{bmatrix} + T_2\frac{2}{3}V_{dc}\begin{bmatrix}\cos\frac{\pi}{3}\\ \sin\frac{\pi}{3}\end{bmatrix} \tag{2.18}$$

Separate real and imaginary parts from the above equation, then

$$T_z\left|V_{ref}\right|\cos\alpha = \frac{2}{3}V_{dc}T_1 + \frac{2}{3}V_{dc}T_2\cos\frac{\pi}{3} \tag{2.19}$$

$$T_z\left|V_{ref}\right|\sin\alpha = \frac{2}{3}V_{dc}T_2\sin\frac{\pi}{3} \tag{2.20}$$

Using equations (2.17) and (2.18) T_1 and T_2 are calculated as follows which are

$$T_1 = \frac{|V_{ref}| T_z \sin\left(\frac{\pi}{3} - \alpha\right)}{\frac{2}{3} V_{dc} \sin\frac{\pi}{3}} \tag{2.21}$$

$$T_2 = \frac{|V_{ref}| T_z \sin\alpha}{\frac{2}{3} V_{dc} \sin\frac{\pi}{3}} \tag{2.22}$$

$$T_0 = T_z - T_1 + T_2 \tag{2.23}$$

ii. Calculation of $T_1, T_2 and T_0$ in any sector:

$$T_z |V_{ref}| \begin{bmatrix} \cos\alpha \\ \sin\alpha \end{bmatrix} = T_1 \frac{2}{3} V_{dc} \begin{bmatrix} \cos(n-1)\frac{\pi}{3} \\ \sin(n-1)\frac{\pi}{3} \end{bmatrix} + T_2 \frac{2}{3} V_{dc} \begin{bmatrix} \cos\frac{n\pi}{3} \\ \sin\frac{n\pi}{3} \end{bmatrix} \tag{2.24}$$

Separate real and imaginary parts from the above equation, then

$$T_z |V_{ref}| \cos\alpha = \frac{2}{3} V_{dc} T_1 \cos(n-1)\frac{\pi}{3} + \frac{2}{3} V_{dc} T_2 \cos\frac{n\pi}{3} \tag{2.25}$$

$$T_z |V_{ref}| \sin\alpha = \frac{2}{3} V_{dc} T_1 \sin(n-1)\frac{\pi}{3} + \frac{2}{3} V_{dc} T_2 \sin\frac{n\pi}{3} \tag{2.26}$$

Using equations (2.23) and (2.24) T_1 and T_2 are calculated as follows which are

$$T_1 = \frac{\sqrt{3} T_z |V_{ref}| \sin\left(\frac{n\pi}{3} - \alpha\right)}{V_{dc}} \tag{2.27}$$

$$T_2 = \frac{\sqrt{3}T_z \left|V_{ref}\right| \sin\left(\alpha - \frac{(n-1)\pi}{2}\right)}{V_{dc}} \tag{2.28}$$

$$T_0 = T_z - T_1 - T_2 \tag{2.29}$$

Where, n = 1 to 6 (i.e sector 1 to 6) and $0 \le \alpha \le \frac{\pi}{3}$

2.8 Calculation of switching time of each switching device (S1 TO S6):

The following table shows the switching sequence corresponds to each sector. For each cycle there are 7 switching states in each sector. The odd sector numbers travels in anti-clockwise direction and even sector numbers travels in clockwise direction. The following table represents the switching sequence each sector.

Table-2.2: Switching sequence of the modulation

Sector no:	Switching sequence
1	$\bar{V}_0 - \bar{V}_1 - \bar{V}_2 - \bar{V}_7 - \bar{V}_2 - \bar{V}_1 - \bar{V}_0$
2	$\bar{V}_0 - \bar{V}_3 - \bar{V}_2 - \bar{V}_7 - \bar{V}_2 - \bar{V}_3 - \bar{V}_0$
3	$\bar{V}_0 - \bar{V}_3 - \bar{V}_4 - \bar{V}_7 - \bar{V}_4 - \bar{V}_3 - \bar{V}_0$
4	$\bar{V}_0 - \bar{V}_5 - \bar{V}_4 - \bar{V}_7 - \bar{V}_4 - \bar{V}_5 - \bar{V}_0$
5	$\bar{V}_0 - \bar{V}_5 - \bar{V}_6 - \bar{V}_7 - \bar{V}_6 - \bar{V}_5 - \bar{V}_0$
6	$\bar{V}_0 - \bar{V}_1 - \bar{V}_7 - \bar{V}_7 - \bar{V}_6 - \bar{V}_1 - \bar{V}_0$

In sector-1 the switching states sequence is $\bar{V}_0 - \bar{V}_1 - \bar{V}_2 - \bar{V}_7 - \bar{V}_2 - \bar{V}_1 - \bar{V}_0$. Here sampling time period is equal to the switching time period T_s, which is divided among the 7 switching states, out of which three are zero vectors.

$$T_z = \frac{T_0}{4} + \frac{T_1}{2} + \frac{T_2}{2} + \frac{T_0}{4} + \frac{T_2}{2} + \frac{T_1}{2} + \frac{T_0}{4} \tag{2.30}$$

The following figure 4 shows the switching pulse pattern in all the sectors. The following symmetrical pulse patterns gives the less harmonics. Based on the symmetric pulses waveforms switching times of all the switching devices in all the sectors are derived. Table-2 represents the switching times of the inverter in each sector

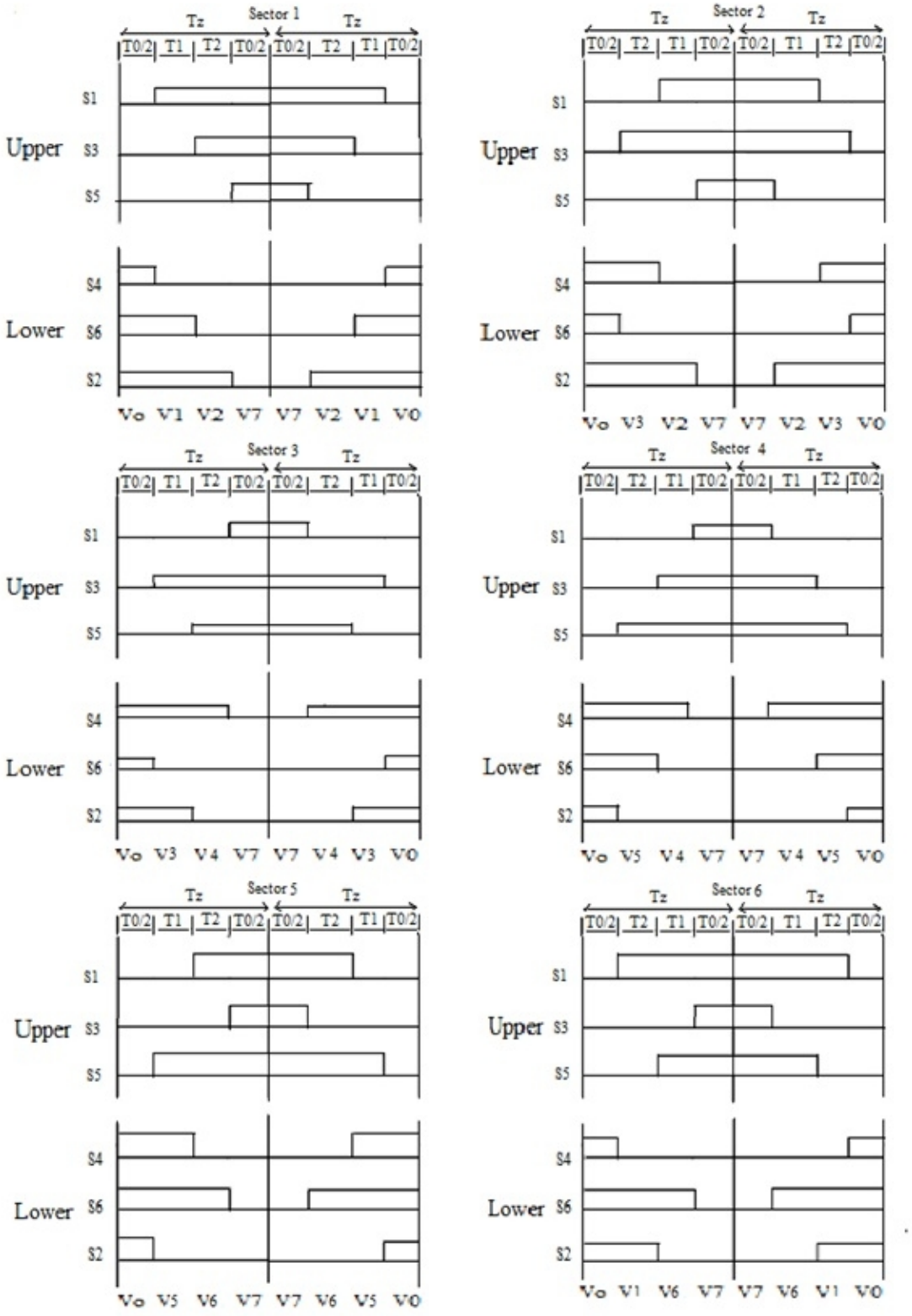

Fig2.5: Switching signal derivation for a period from voltage vectors in all the sectors

Table 2.3. Switching times in each sector

Sector no	Rotor position in each sector	Upper switching Devices(S1, S3, S5)	Lower switching Devices(S4, S6, S2)
1	$0^0 \le \theta \le 60^0$	$S_1 = T_1 + T_2 + \frac{T_0}{2};$ $S_3 = T_2 + \frac{T_0}{2};$ $S_5 = \frac{T_0}{2};$	$S_4 = \frac{T_0}{2};$ $S_6 = T_1 + \frac{T_0}{2};$ $S_2 = T_1 + T_2 + \frac{T_0}{2};$
2	$60^0 \le \theta \le 120^0$	$S_1 = T_1 + \frac{T_0}{2};$ $S_3 = T_1 + T_2 + \frac{T_0}{2};$ $S_5 = \frac{T_0}{2};$	$S_4 = T_2 + \frac{T_0}{2};$ $S_6 = \frac{T_0}{2};$ $S_2 = T_1 + T_2 + \frac{T_0}{2};$
3	$120^0 \le \theta \le 180^0$	$S_1 = \frac{T_0}{2};$ $S_3 = T_1 + T_2 + \frac{T_0}{2};$ $S_5 = T_2 + \frac{T_0}{2};$	$S_4 = T_1 + T_2 + \frac{T_0}{2};$ $S_6 = \frac{T_0}{2};$ $S_2 = T_1 + \frac{T_0}{2};$
4	$180^0 \le \theta \le 240^0$	$S_1 = \frac{T_0}{2};$ $S_3 = T_1 + \frac{T_0}{2};$ $S_5 = T_1 + T_2 + \frac{T_0}{2};$	$S_4 = T_1 + T_2 + \frac{T_0}{2};$ $S_6 = T_2 + \frac{T_0}{2};$ $S_2 = \frac{T_0}{2};$
5	$240^0 \le \theta \le 300^0$	$S_1 = T_2 + \frac{T_0}{2};$ $S_3 = \frac{T_0}{2};$ $S_5 = T_1 + T_2 + \frac{T_0}{2};$	$S_4 = T_1 + \frac{T_0}{2};$ $S_6 = T_1 + T_2 + \frac{T_0}{2};$ $S_2 = \frac{T_0}{2};$

6	$300^0 \le \theta \le 360^0$	$S_1 = T_1 + T_2 + \frac{T_0}{2};$ $S_3 = \frac{T_0}{2};$ $S_5 = T_1 + \frac{T_0}{2};$	$S_4 = \frac{T_0}{2};$ $S_6 = T_1 + T_2 + \frac{T_0}{2};$ $S_2 = T_2 + \frac{T_0}{2};$

Chapter-3

Introduction to the BLDC Motor Drive

3.1 Introduction

Brushless Direct Current Motors (BLDC) are using in many applications because of the controlling is simple. It is electronically commutated motor. Therefore there is no usage brushes, the maintenance cost is less, and the reliability is more. BLDC motors are available in compact size with wide speed ranges. If the shape of the back emf induced in the stator of the armature coils is trapezoidal and the phase current is rectangular, then motor gives zero ripple torque. But in practical the electromagnetic torque in the BLDC motor contains ripple content, due to the commutation effect, and the rotor position angle. This is only the drawback of the motor. BLDC motor is looking like a permanent magnet synchronous motor i.e it has three phase armature winding placed on the stator. Each winding is displaced by 120 degrees apart. The rotor is surface mounted permanent magnet with number of pole pairs. The torque-speed characteristics of the BLDC motor is same as the Brushed DC motor. That's this motor is called as BLDC motor. The copper saving is more in the BLDC motor than the PMSM motor for the same power rating of the both the motors. The trapezoidal shape of the back emf of the BLDC motor is due to the distribution of the coils on the stator winding.

3.2 Principle operation of BLDC motor

The principle operation of BLDC motor and Brushed DC motor is same. In Brushed DC motor the feedback is mechanical commutator, but in BLDC motor the feedback is given feedback sensors which are hall sensors or optical encoders.

The principle of the hall sensors is that whenever a current carrying conductor is placed in the magnetic field it produces a force so that the emf induced on the two sides of the conductors. The hall sensors placed in the stator of the BLDC motor gives low or high signal when the rotor rotates and moves near to the sensor, which gives the position of the rotor.

The DC voltage is applied to the motor through three phase voltage source inverter (VSI), so that the stator coils are excited and due the interaction of stator flux and the rotor flux the starts rotating. To maintain this rotation the orientation of the magnetic field should be rotated sequentially in either clockwise direction or in anti-clockwise direction.

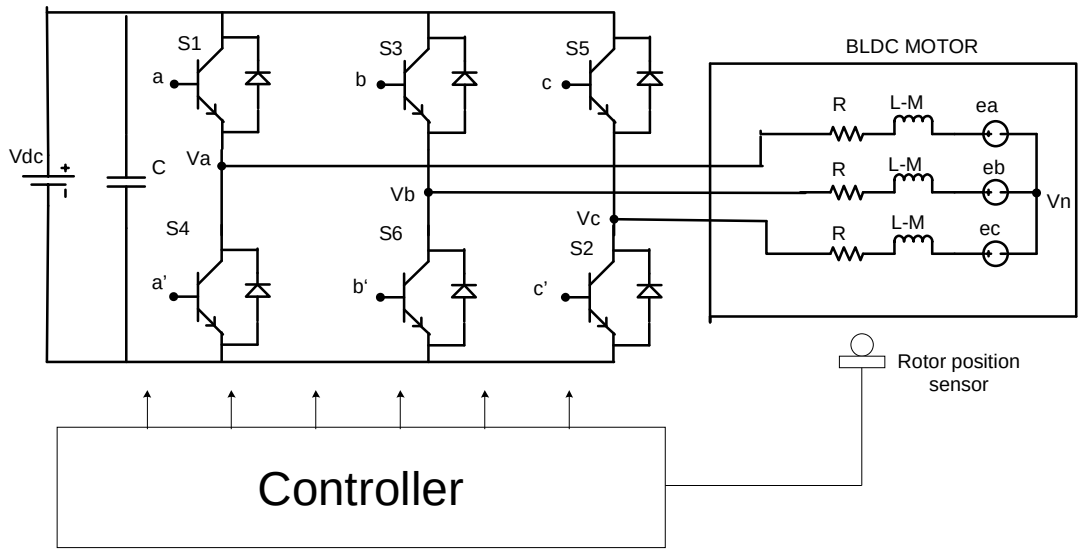

Fig3.1: Three phase voltage source inverter with BLDC motor

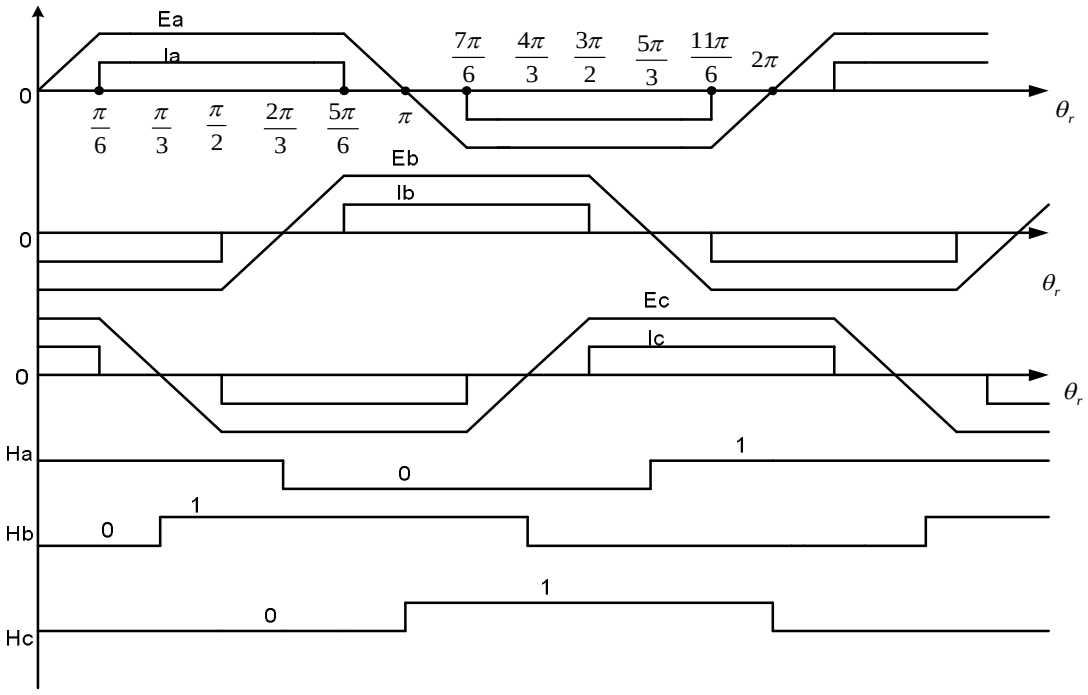

Fig3.2: back emf, phase current waveforms and hall sensor signals

3.3 Energization sequence of the BLDC Motor

In a three phase BLDC motor only two phase windings are energized by a three phase voltage source inverter at a time. The energization sequence is depends on the rotor position of the motor. Suppose the motor is rotating in anti-clockwise direction. Then the sequence of the windings energized in such a way that the motor rotates in the anti-clockwise direction, the energization sequence during a complete cycle is ac-bc-ba-ca-cb-cb. Each sequence conducting interval is 60 degree. Therefore the commutation is done at every 60 degrees interval.

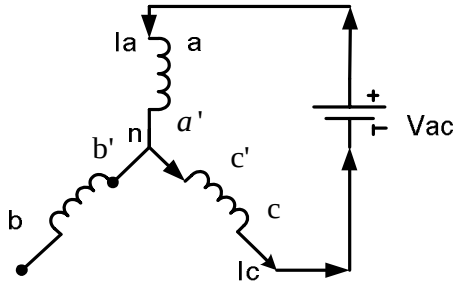

a) $0^0 \le \theta_r \le 60^0$

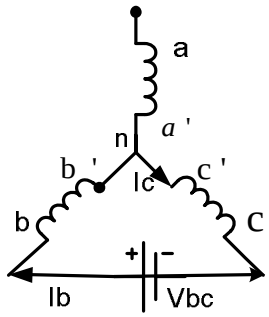

b) $60^0 \le \theta_r \le 120^0$

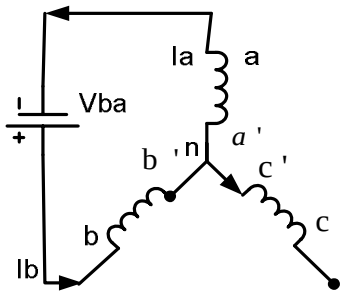

c) $120^0 \le \theta_r \le 180^0$

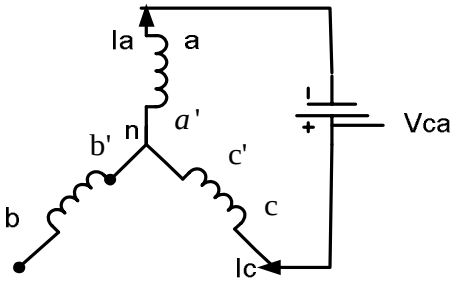

d) $180^0 \le \theta_r \le 240^0$

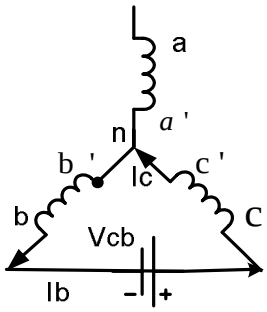

e) $240^0 \le \theta_r \le 300^0$

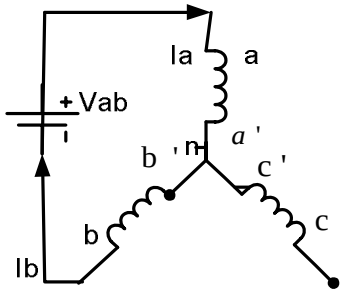

f) $300^0 \le \theta_r \le 360^0$

Fig3.3: energization sequence of BLDC motor

3.4 Dynamic model of BLDC Motor

BLDC Motor has star connected three phase winding and rotor has permanent magnet. The induced currents in the rotor cab be neglected no damper windings are modelled, because both the magnet stainless steel retaining sleeves have high sensitivity. The mathematical model of the BLDC Motor is shown in the figure

$$V_{ax} = R_1 i_{ax} + L_s \frac{di_{ax}}{dt} + M \frac{di_{bx}}{dt} + M \frac{di_{cx}}{dt} + e_a \tag{3.1}$$

$$V_{bx} = R_1 i_{bx} + M \frac{di_{ax}}{dt} + L_s \frac{di_{bx}}{dt} + M \frac{di_{cx}}{dt} + e_b \tag{3.2}$$

$$V_{cx} = R_1 i_{cx} + M \frac{di_{ax}}{dt} + M \frac{di_{bx}}{dt} + L_s \frac{di_{cx}}{dt} + e_c \tag{3.3}$$

Where $V_{ax}, V_{bx}\ and\ V_{cx}$ are stator phase voltages, R_1 is the stator per phase resistance, $i_{ax}, i_{bx}\ and\ i_{cx}$ are the per phase stator currents, L_s is the self-inductance of the each stator winding and M is mutual inductance between any two windings. Let us assume that leakage resistance (R_1) and self-inductance (L_s) of three windings are equal and mutual inductance (M) between the any two windings are equal.

The back EMF $e_a, e_b, and\ e_c$ are trapezoidal in shape

$$\begin{pmatrix} e_a \\ e_b \\ e_c \end{pmatrix} = \omega_x \lambda_x \begin{pmatrix} f_{ax}(\theta_r) \\ f_{bx}(\theta_r) \\ f_{cx}(\theta_r) \end{pmatrix} \tag{3.4}$$

Where ω_x is rotor speed in radians per second, θ_r is rotor position in radians and λ_x is the flux linkage of the rotor and the functions $f_{ax}(\theta_r)$, $f_{bx}(\theta_r)$ and $f_{cx}(\theta_r)$ have the same trapezoidal shape as $e_a, e_b\ and\ e_c$ with a peak amplitude of ± 1.

$$f_{ax}(\theta_r) = \begin{cases} 1, & 0 \le \theta_r \le \pi/3 \\ (\pi/2 - \theta_r)6/\pi, & \pi/3 \le \theta_r \le 2\pi/3 \\ -1, & 2\pi/3 \le \theta_r \le \pi \\ -1, & \pi \le \theta_r \le 4\pi/3 \\ (\theta_r - 3\pi/2)6/\pi, & 4\pi/3 \le \theta_r \le 5\pi/3 \\ 1, & 5\pi/3 \le \theta_r \le 2\pi \end{cases} \tag{3.5}$$

Similarly

$$f_{bx} = f_{ax}\left(\theta_r - 2\pi/3\right) \tag{3.5}$$

$$f_{cx} = f_{ax}\left(\theta_r + 2\pi/3\right) \tag{3.6}$$

For a balanced star connected three phase winding current is

$$i_{ax} + i_{bx} + i_{cx} = 0 \tag{3.7}$$

Substitute equation (3.4) in equations (3.1, 3.2, 3.3)

$$\begin{pmatrix} V_{ax} \\ V_{bx} \\ V_{cx} \end{pmatrix} = \begin{pmatrix} R_1 & 0 & 0 \\ 0 & R_1 & 0 \\ 0 & 0 & R_1 \end{pmatrix} \begin{pmatrix} i_{ax} \\ i_{bx} \\ i_{cx} \end{pmatrix} + \begin{pmatrix} L_s - M & 0 & 0 \\ 0 & L_s - M & 0 \\ 0 & 0 & L_s - M \end{pmatrix} p \begin{pmatrix} i_{ax} \\ i_{bx} \\ i_{cx} \end{pmatrix} + \begin{pmatrix} e_a \\ e_b \\ e_c \end{pmatrix} \tag{3.8}$$

The electromagnetic torque equation is given by

$$T_e = \left[e_a i_{ax} + e_b i_{bx} + e_c i_{cx}\right] / \omega_x \tag{3.9}$$

The equation of motion for a simple system with inertia J, friction coefficient-B, and load torque T_l is

$$J\frac{d\omega_x}{dt} + B\omega_x = T_e - T_l \tag{3.10}$$

And electrical rotor speed and rotor position are related by

$$\frac{d\theta_r}{dt} = \frac{p}{2}\omega_x \tag{3.11}$$

Combining all the relevant equations, the system in state space form is

$$\dot{x} = Ax + Bu \tag{3.12}$$

$$y = Cx \tag{3.13}$$

Where

$$\dot{x} = \begin{bmatrix} i_{ax} & i_{bx} & i_{cx} & \omega_x & \theta_r \end{bmatrix}^T \tag{3.14}$$

$$y = \begin{pmatrix} i_{ax} & i_{bx} & i_{cx} & \omega_x & \theta_r \end{pmatrix}^T \tag{3.15}$$

$$u = \begin{pmatrix} V_{ax} & V_{bx} & V_{cx} & T_l \end{pmatrix}^T \tag{3.16}$$

$$A = \begin{pmatrix} \frac{-R_1}{L_s - M} & 0 & 0 & \frac{-\lambda_x}{L_s - M} f_{ax}(\theta_r) & 0 \\ 0 & \frac{-R_1}{L_s - M} & 0 & \frac{-\lambda_x}{L_s - M} f_{bx}(\theta_r) & 0 \\ 0 & 0 & \frac{-R_1}{L_s - M} & \frac{-\lambda_x}{L_s - M} f_{cx}(\theta_r) & 0 \\ \frac{\lambda_x}{J} f_{ax}(\theta_r) & \frac{\lambda_x}{J} f_{bx}(\theta_r) & \frac{\lambda_x}{J} f_{cx}(\theta_r) & \frac{-B}{J} & 0 \\ 0 & 0 & 0 & \frac{p}{2} & 0 \end{pmatrix} \tag{3.17}$$

$$B = \begin{pmatrix} \frac{1}{L_s - M} & 0 & 0 & 0 \\ 0 & \frac{1}{L_s - M} & 0 & 0 \\ 0 & 0 & \frac{1}{L_s - M} & 0 \\ 0 & 0 & 0 & \frac{-1}{J} \end{pmatrix} \tag{3.18}$$

$$C = \begin{pmatrix} 1 & 0 & 0 & 0 \\ 0 & 1 & 0 & 0 \\ -1 & 1 & 0 & 0 \\ 0 & 0 & 1 & 0 \\ 0 & 0 & 0 & 1 \end{pmatrix} \tag{3.19}$$

3.5 PULSATING TORQUE IN BLDC MOTOR

In BLDC Motor the stator is star connected three phase armature winding, which are labelled as aa', bb' and cc'. Rotor is permanent magnet, considering one pole pair which have north and south poles. For easy analysis of torque production in BLDC Motor consider only a-a' winding is energized so that the current i_a flowing in the a-a' winding is under the influence of the rotor magnetic flux density $B_{m.}$ Applying Lorentz force equation to the current flowing through the a and a' sides of the winding having length of l meters gives

$$F = i_a(\vec{l} \times \vec{B}_m) \tag{3.20}$$

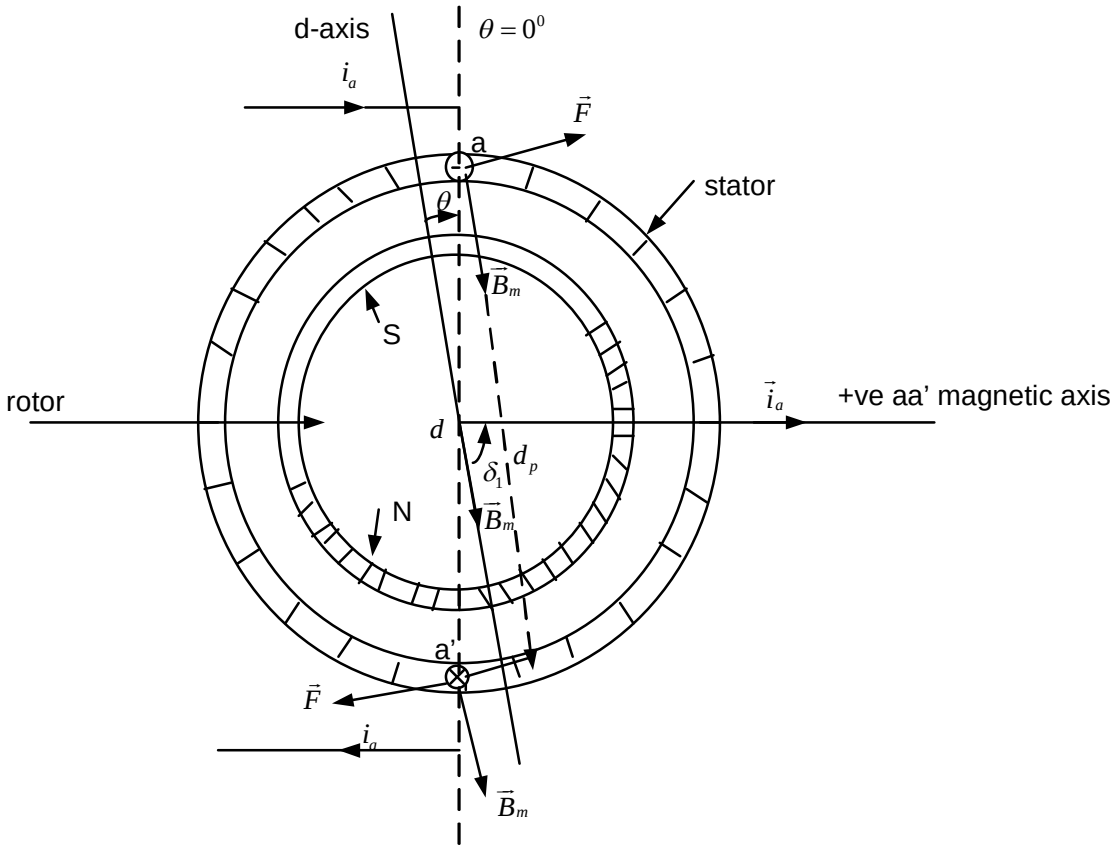

Fig.3.4: Schematic diagram of two pole BLDC motor with one winding excitation

Where $\vec{l}$ is the displacement vector in the direction of current i_a. If $\vec{B}_m$ and $\vec{l}$ are orthogonal, then

$$F = B_m i_a l \vec{j} \tag{3.21}$$

Where $\vec{J}$ is the vector perpendicular to the plane contained by $\vec{B}_{\mathrm{m}}$ and $\vec{l}$.

Two forces with opposite direction are acting on the winding a-a' and which are separated by perpendicular distance dp. Then electromagnetic torque developed on the aa' winding is given by

$$Teaa' = B_m i_a l\, d \sin \delta 1\, \vec{r} \tag{3.22}$$

Where d is the diameter of the winding a-a', $\delta 1 = 90 - \theta$ and $\vec{r}$ is a unit vector.

Now winding aa' having N turns, and area $A = ld$, $\emptyset_m = B_m A \; and \; \lambda_m = N\phi_m$

Substitute above equations in equation (3) then electromagnetic torque developed by winding aa' is given by

$$Teaa' = \lambda_m i_a \sin \delta 1\, \vec{r} \tag{3.23}$$

Where λ_m is the peak flux linkage of the permanent magnet rotor. And $\delta 1$ is the angle between the vectors $\vec{\lambda} m$ and $\vec{\imath} a$, and also $\delta 1$ is the function of the rotor position

Equation (4) can be represented as in the form

$$Teaa' = \vec{\lambda}_m \mathrm{X}\, \vec{\imath}_a \tag{3.24}$$

In the equation (5) the vectors $\lambda_m and \; i_a$ are constant. The pulsating torque produced in the BLDC motor due to the angle $\delta 1$ which is varying sinusoidally.

3.6 Torque production due to two winding energization

In BLDC Motor two stator windings are energized out of three windings, so we have to find the electromagnetic torque due to two winding energization. Assume that the motor is rotating in anti-clockwise direction, so the electromagnetic torque developed for rotor position range $0^0 \leq \theta \leq 60^0$ for when phase winding pair ac is energized using the vector diagram of figure.

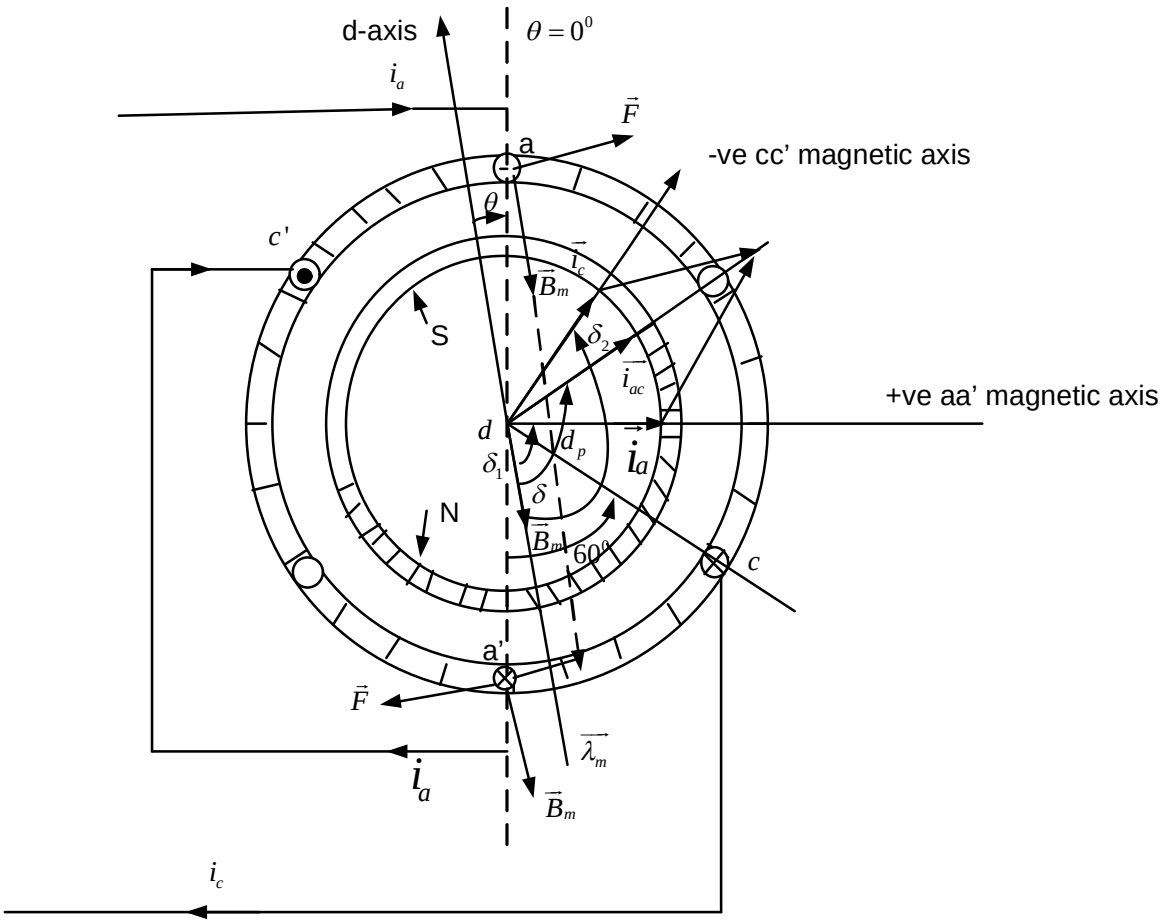

Fig.3.5: Schematic diagram of the BLDC motor with two winding excitation

The phase current i_a is flowing through the winding a to a', so it establishes magnetis current vector $\vec{\imath}_a$ along the positive magnetic axis of winding aa'. And phase current i_c is flowing through winding c' to c, magnetic current vector $\vec{\imath}_c$ along the negative magnetic axis of winding cc' as shown in the figure. So these two magnetic current vectors $\vec{\imath}_a$ and $\vec{\imath}_c$ makes an angles $\delta 1 \; and \; \delta 2$ with the peak flux linkage vector of the rotor magnet $\overrightarrow{\lambda_m}$. The two phase windings aa' and cc' are connected in series, so the vector current magnitudes

$$|\vec{\imath}_a| = |\vec{\imath}_c| \tag{3.25}$$

These two currents are added vectorially so the resultant current $\vec{\imath}_{ac}$ that makes an δ with peak flux linkage vector $\vec{\lambda}_m$ due to the rotor. Now the rotor turns in anticlockwise direction, the angle θ increases from 0^0 electrical degree to 60^0 electrical degrees, i.e the torque angle decreases from 120^0 electrical degrres to 60^0 electrical degrees.

The following equation gives electromagnetic torque development due to the interaction rotor peak flux linkage vector $\overrightarrow{\lambda_m}$ and the resultant winding pair current $\vec{\imath}_{ac}$.

$$\vec{T}_e = \vec{\lambda}_m \times \vec{\imath}_{ac} = (\vec{\lambda}_m \times \vec{\imath}_a) + (\vec{\lambda}_m \times \vec{\imath}_c) \quad (3.26)$$

$$T_e = \lambda_m i_{ac} \sin\delta = \lambda_m i_a \sin\delta_1 + \lambda_m i_c \sin\delta_2 \quad (3.27)$$

Where $\delta_1 = 90^0 - \theta, \delta_2 = 150^0 - \theta, and\ \delta = 120^0 - \theta$;

Therefore permanent magnet rotor develops torque and the rotor rotates in the anti-clockwise direction, then the angles $\delta, \delta_1\ and\ \delta_2$ are decreases as the rotor position θ increases. From equation (8) the electromagnetic torque during the rotor position $0^0 \leq \theta \leq 60^0$ is maximum at $\theta = 30^0$ i.e $\delta = 90^0$ and at $\theta = 0^0, 60^0$ torque is minimum.

At $\theta = 60^0$ winding bb' will be energized, i.e. during the rotor position range $60^0 \leq \theta \leq 120^0$ the resultant stator current will be $\vec{\imath}_{bc}$ that will make angle δ with the peak flux linkage vector $\vec{\lambda}_m$. Therefore the electromagnetic torque developed during the rotor position range $60^0 \leq \theta \leq 120^0$ is given by

$$T_e = \lambda_m i_{bc} \sin\delta \quad (3.28)$$

Where $\delta = 180^0 - \theta$;

The following tabular form gives the electromagnetic torque developed in the BLDC Motor over a cycle of anti-clockwise direction of motor. Hence this machine is characterised as a pulsating torque machine.

Rotor position range	Phase sequence	Developed torque
$0^0 \leq \theta \leq 60^0$	Ac	$T_e = \lambda_m i_{ac} \sin(120^0 - \theta)$
$60^0 \leq \theta \leq 120^0$	Bc	$T_e = \lambda_m i_{bc} \sin(180^0 - \theta)$
$120^0 \leq \theta \leq 180^0$	Ba	$T_e = \lambda_m i_{ba} \sin(240^0 - \theta)$
$180^0 \leq \theta \leq 240^0$	Ca	$T_e = \lambda_m i_{ca} \sin(\theta - 120^0)$
$240^0 \leq \theta \leq 300^0$	Cb	$T_e = \lambda_m i_{cb} \sin(\theta - 180^0)$
$300^0 \leq \theta \leq 360^0$	Ab	$T_e = \lambda_m i_{ab} \sin(\theta - 240^0)$

Table-3.1: Electromagnetic torque production in each sector

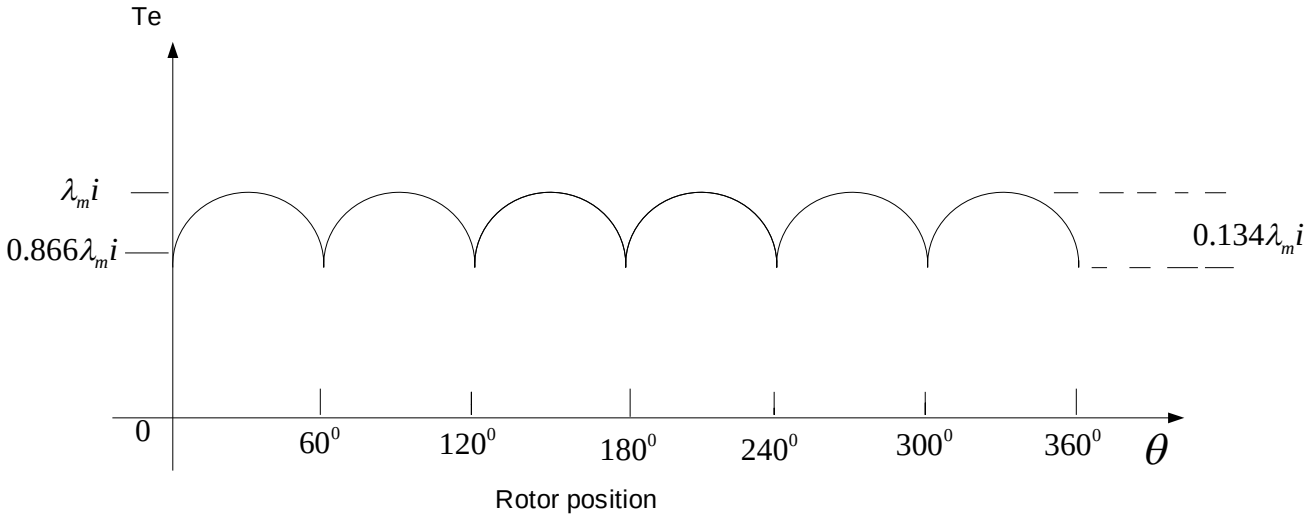

Fig3.6: Pulsating torque in BLDC motor

Chapter-4

Controller design

4.1 Introduction about PID speed controller

The Proportional Integral Derivative (PID) controller is reduces error between the reference value and the actual value. The proportional controller increases the DC gain of the system, integral controller reduces the steady state error and the derivative controller reduces the oscillations and the peak over shoot of the system. The structure of the PID controller is shown in the figure below.

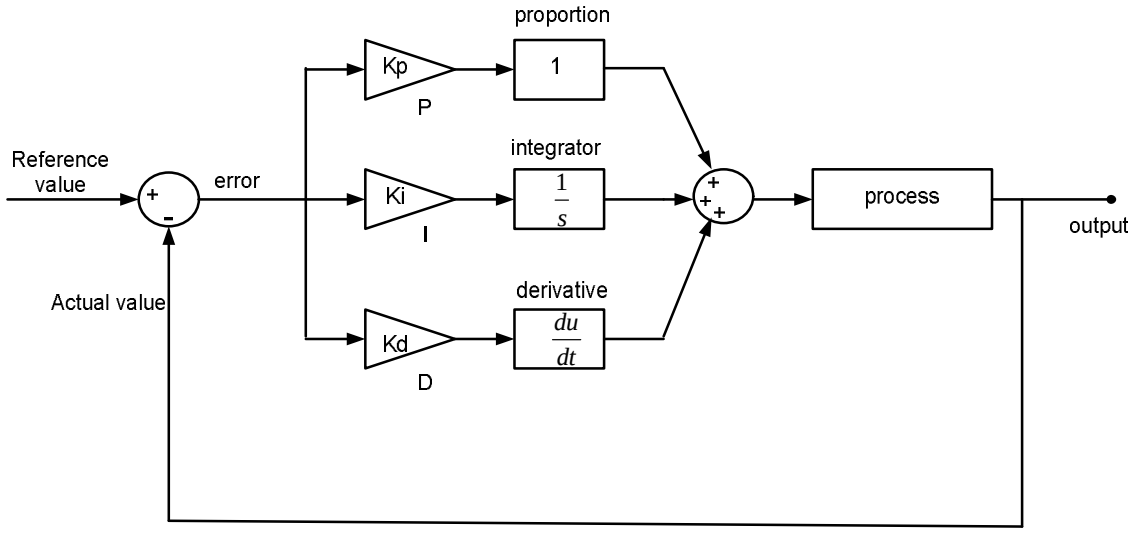

Fig4.1: PID controller for closed loop system

The PID controller equation is

$$e(t) = k_p + \frac{k_i}{s} + k_d s \tag{4.1}$$

(4.2)

$$e(\mathrm{t}) = k_p \left(1 + \frac{1}{T_i s} + T_d s \right) \tag{4.3}$$

Where error $e(\mathrm{t})$ = reference value – actual value,

Ti = integral time constant, Td = derivative time constant.

$$T_i = \frac{k_i}{k_p} \tag{4.4}$$

$$T_d = \frac{k_d}{k_p} \tag{4.5}$$

PID controller is controls the feedback of the process plant and the feedback loops are very important parts of the plant which are controlled by reference value. The error signal s processed by the controller and the process plant and again feedback to the reference value.

4.2 Speed controller design of the BLDC motor

The desired speed can be achieved by using the suitable speed controller. Here we are discussing about the PID controller as the speed controller. Because it can reduce peak overshoot, steady state error, and the settling time by choosing the proper Kp, Ki, and the Kd values. Here the plant transfer function is BLDC motor transfer function. The open loop transfer function of the BLDC motor is the ratio of the speed to the inverter output voltage is

$$G(s) = \frac{\omega_m}{V_{cm}} = \frac{\frac{1}{k_e}}{t_m t_e s^2 + t_m s + 1} \tag{4.6}$$

Where k_e = back emf constant

$$k_e = \left\{ \frac{v - \sec}{rad} \right\}$$

t_m = mechanical time constant

$$t_m = \left\{ \frac{J_r 3R}{k_e k_t} \right\} \tag{4.7}$$

t_e = Electrical time constant

$$t_e = \left\{ \frac{L}{3R} \right\} \tag{4.8}$$

The mechanical time constant is more than the electrical time constant.

k_t = The torque constant

$$k_t = \left\{ \frac{N-m}{A} \right\}$$

R = per phase resistance in ohms,

L = per phase inductance of the stator coils,

ω_m = is the speed of the motor,

J_r = moment of the rotor in kg-cm2.

The speed controller structure of the BLDC motor is shown in the figure

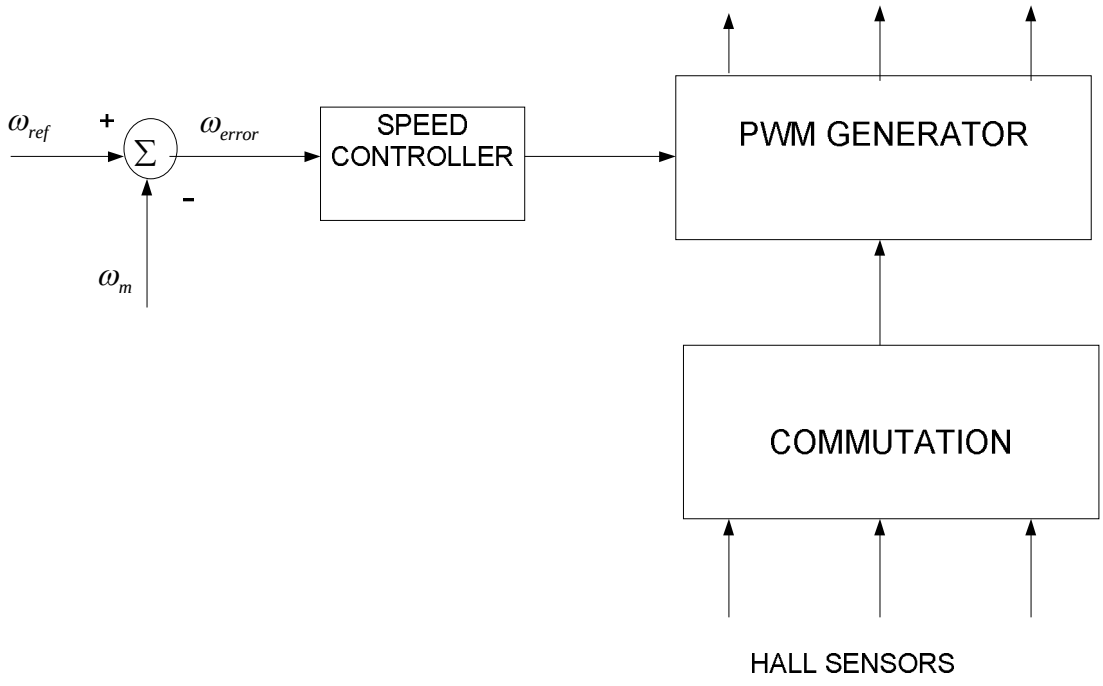

Fig4.2: Speed controller structure of the BLDC motor

The actual speed is sensed and it is given as negative feedback which is compared with the reference speed of the motor. Then the difference is the speed error is given as input to the speed controller. The output of the speed controller is given to the SVPWM inverter which produces the PWM pulses which are multiplied with the commutation sequence, so that only two phase windings are energized at a time by using this commutation sequence and also each switching device is conducting 120 degree. The commutation sequence is generated by applying hall sensor signals to the commutation. Here the speed controller is PID controller There are many methods to tune the Kp, Ki, and the Kd values which are Zigler-Nicholos method, open-loop bode method, the Routh- array method and compensator design techniques.

4.3 The tuning methods of PID controller

There are many ways to tune the Kp, Ki, and the Kd values for the BLDC motor control, those methods are trial and error technique, routh-array technique, cohen-coon technique, Ziegler-Nicholas technique, improved Ziegler- Nicholas technique and the genetic algorithm method etc.

4.4 Zigler-Nicholos method for PID controller design

It is a very easier method for tuning the Kp, Ki, and the Kd values for the BLDC motor control. This method is used for finding the open loop transfer function of the system. There are two parameter in the Ziegler- Nicholas which are delay time and the time constant, based on the these two parameters the Kp, Ki, and the Kd values will be determined. These parameters can be determined by the applying tangents to the open loop step response of the system. In this method first we have to find the open loop response by applying step input to the system, after that we have to draw the tangents to the open loop step response of the horizontal axis and the points of inflections. The following diagram represents the parameters of the Ziegler Nicholas tuning method in the open loop step response system shown in the figure.

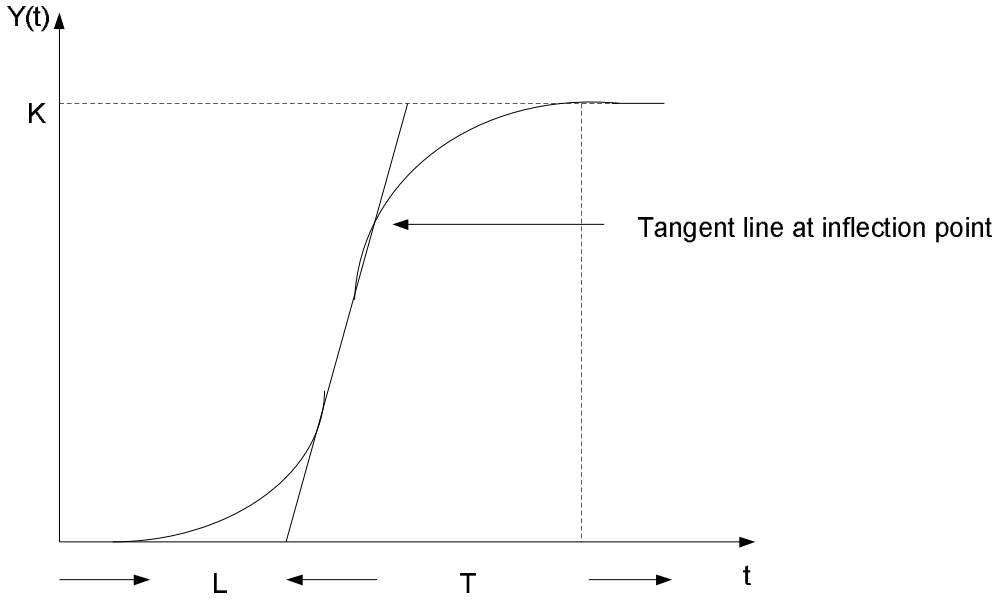

Fig4.3: 'S' shaped curve

The above curve gives the K value on the output axis, and the delay time L, time constant T can be determined on the time axis.

Then the approximate transfer function of the system with these values is

$$G(s) = \frac{Ke^{-Ls}}{1+sT} \tag{4.9}$$

Based on the following tabular form which is suggested by Ziegler Nicholas, the Kp, Ki, and the Kd values will be determined.

S.no	Controller type	Kp	Ti	Td
1	P	T/L	∞	0
2	PI	0.9×T/L	L/0.3	0
3	PID	1.2×T/L	2×L	0.5×L

Table-4.1: Parameters of the PID controller

From the table-5 gives the Kp, Ti, and the Td values for PID controller are

$$Kp = 1.2 \times T/L \tag{4.10}$$

$$Ti = 2 \times L \tag{4.11}$$

$$Td = 0.5 \times L \tag{4.12}$$

Substitute equations (4.4), (4.5) in the (4.11), (4.12) respectively, then

$$Ki = Kp \times Ti \tag{4.13}$$

$$Kd = Kp \times Td \tag{4.14}$$

Chapter-5

Simulation Results

5.1 Simulation Results with Space Vector PWM Technique

The results of SVPWM inverter is shown below

V_{dc} = 400 V

Inverter frequency = 50 Hz

Switching Frequency = 10000 Hz

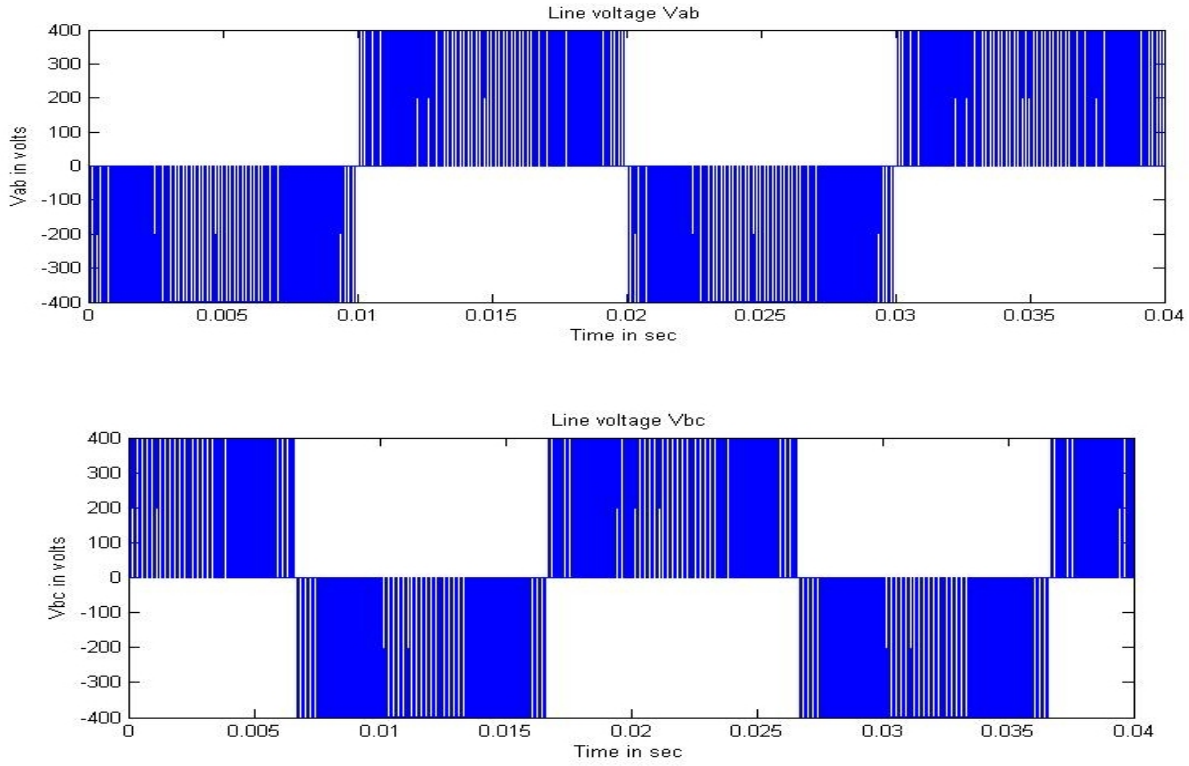

Fig.5.1 Line to Line Voltage output

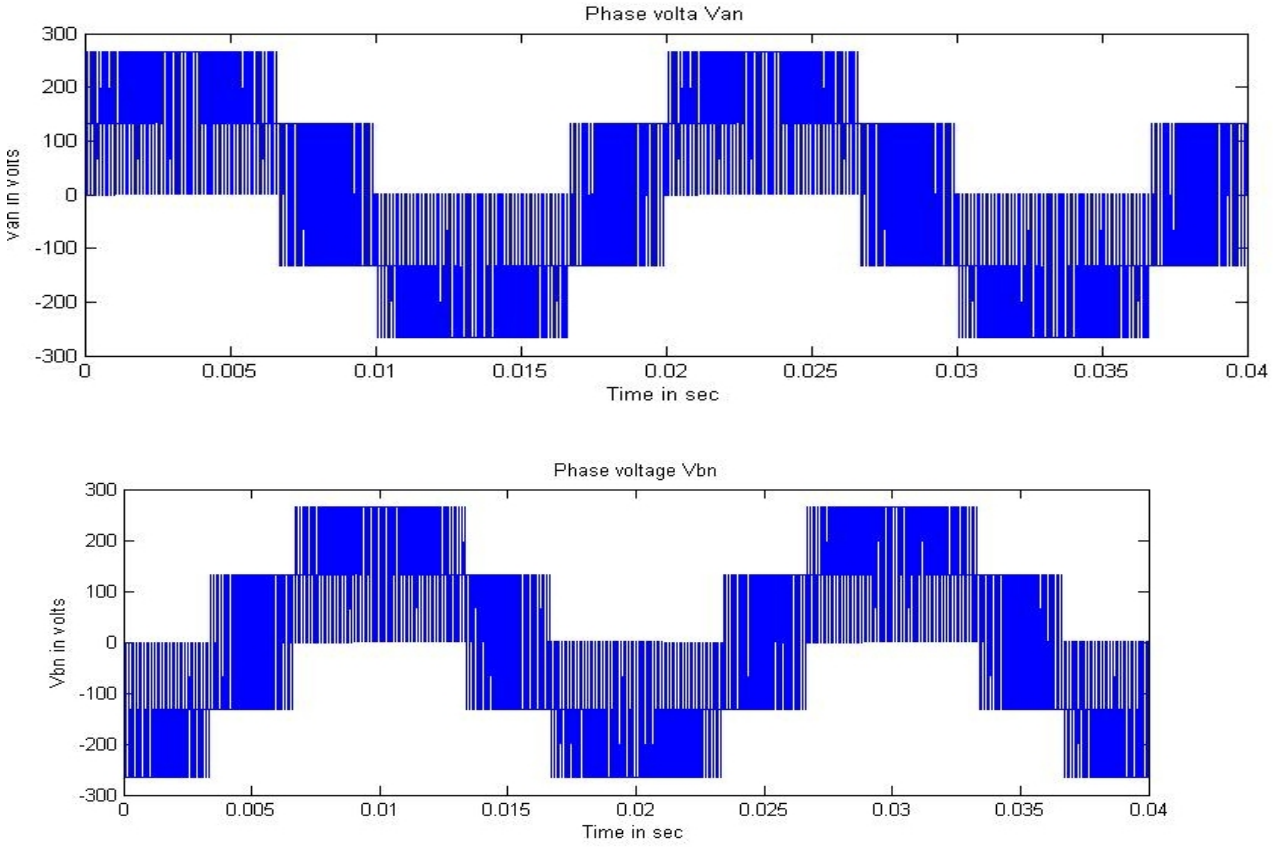

Fig.5.2 Phase Voltage output

5.2. Simulation Results with Commutation Sequence

In this inverter is work in $2\pi/3$ angle switched on mode. Each switch in the inverter is on for 120 degree. The output results are shown.

Specifications	Value
Resistance	3 Ω
Inductance	9 mH
Rotor inertia	0.0009 kg m^2
Friction constant	0.001

Table-5.1 Motor Specifications

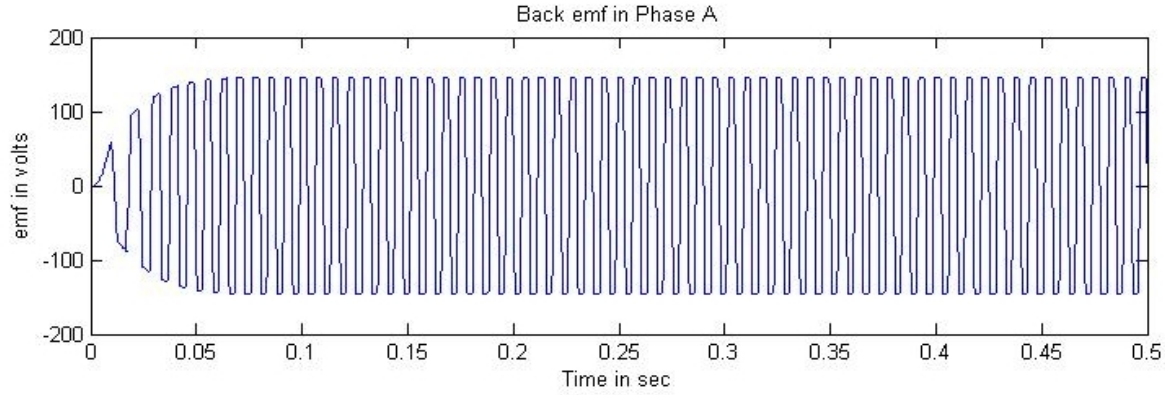

Fig 5.3.Back emf in stator

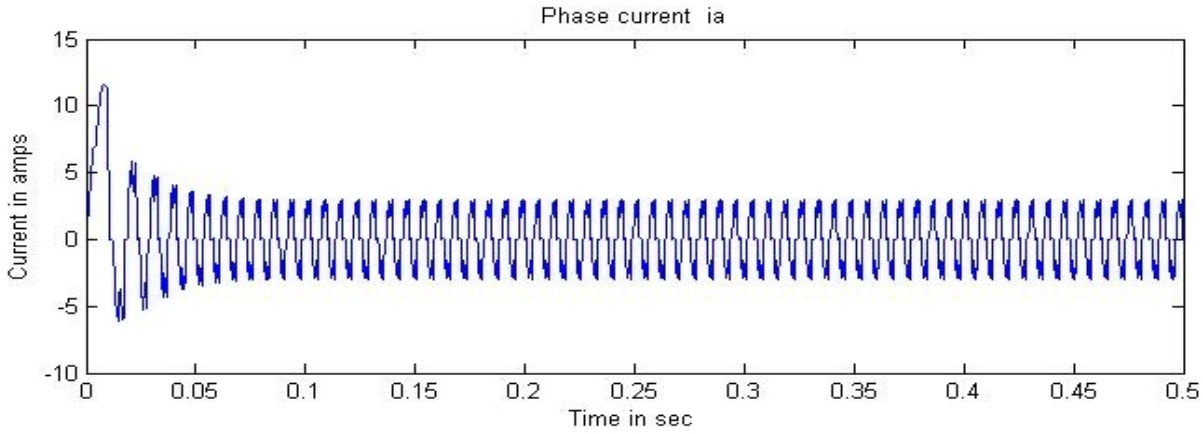

Fig 5.4. Current in the Stator

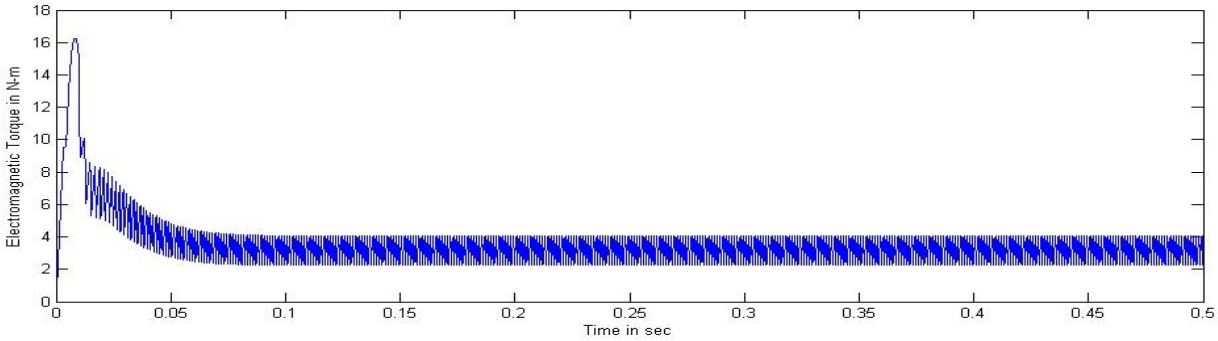

Fig 5.5.electromagnetic torque in N-m

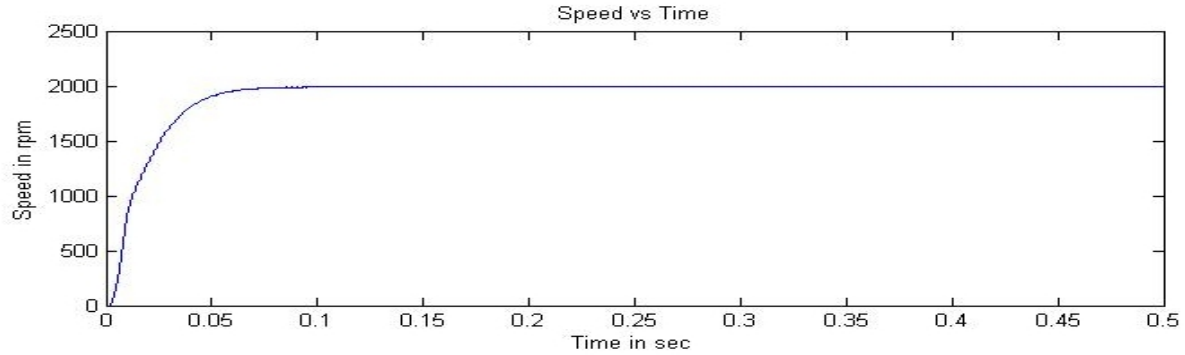

Fig 5.6. Speed response in rpm verse Time

6.3 Simulation Results with SVPWM

SVPWM technique in used to control the duty ratio of switches of the three phase inverter. A PI controller is used to control the speed of BLDC motor drive. The value of proportional and integral gain is 0.015 and 12 respectively. The simulation results are shown below.

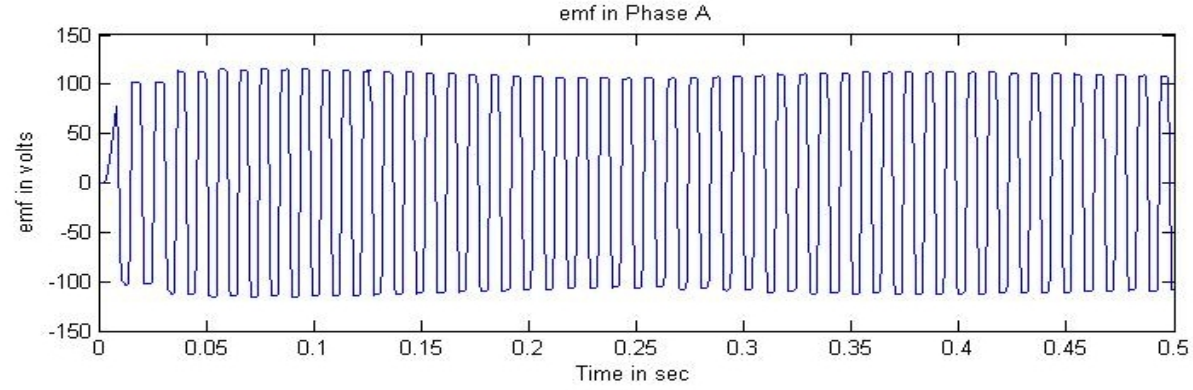

Fig 5.7. Emf in stator winding

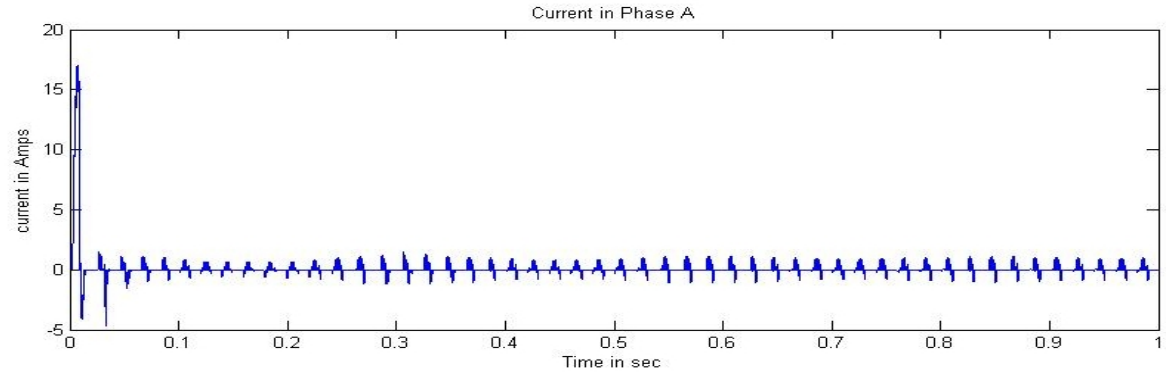

Fig 5.8. Current in the stator

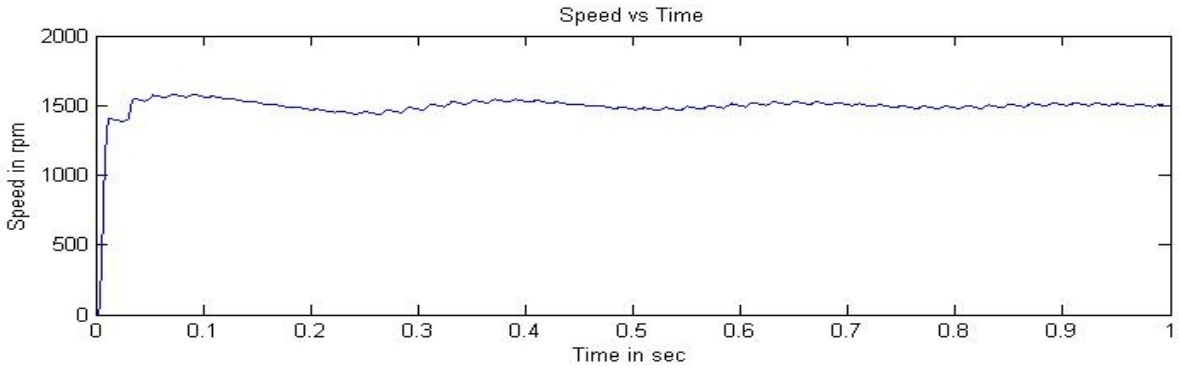

Fig 5.9.Speed response in rpm

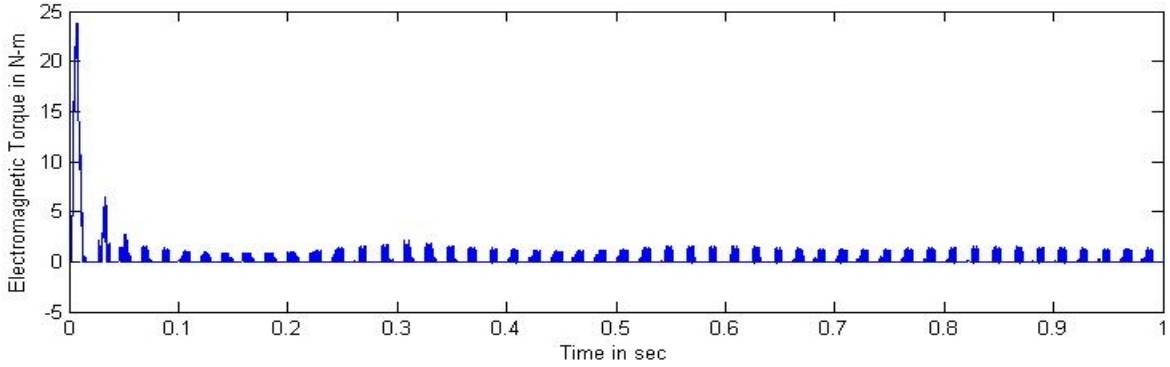

Fig 5.10. Electromagnetic Torque in N-m

Chapter-6

Conclusions and the scope of the future work

6.1 Conclusion

The modelling and simulation of the complete drive system is described in this thesis. Using MATLAB Simulink software SVPWM inverter was implemented. It was observed that the SVPWM inverter utilizes the DC link voltage of 15.5% more when compared with the SPWM inverter. The commutation sequence is multiplied with the SVPWM pulses so that the BLDC motor achieves rectangular current. The speed control of BLDC motor with 120 degree switch on mode inverter and using SVPWM inverter was implemented in MATLAB Simulink software. With SVPWM inverter we achieves a better control over voltage and current supplied to the motor.

6.2 Future scope

To implement the speed control of BLDC motor using SVPWM inverter using Arduino micro controller. Speed control of BLDC motor with fuzzy logic controller. To implement the speed control of BLDC motor with SVPWM inverter using Digital signal processor board.

Bibliography

[1] Yedamale, Padmaraja. "Brushless DC (BLDC) motor fundamentals." *Microchip Technology Inc* (2003): 20.

[2] Park, Sung-Jun, Han Woong Park, Man Hyung Lee, and Fumio Harashima. "A new approach for minimum-torque-ripple maximum-efficiency control of BLDC motor." *Industrial Electronics, IEEE Transactions on* 47, no. 1 (2000): 109-114.

[3] Jahns T. M., Torque Production in Permanent Magnet Synchronous Motor Drives with Rectangular Current Excitation, IEEE Trans. Ind. Applicat., vol. 20, pp. 803–813, July/June 1984.

[4] Hernandez, Agustina, Ruben Tapia, Omar Aguilar, and Abel Garcia. "Comparison of SVPWM and SPWM techniques for back to back converters in PSCAD." In *Proceedings of the World Congress on Engineering and Computer Science*, vol. 1. 2013.

[5] Li Rong, Liu Weiguo, Liu Xiangyang, “A Novel PM BLDC Motors Topology for Extending Constant Power Region,” 33rd Annual Conference of the IECON, Nov. 5-8 2007.

[6] P. Pillay and R. Krishnan, “Modelling analysis and simulation of a high performance, vector controlled, permanent magnet synchronous motor drive,” presented at the IEEE IAS

Annual. Meeting, Atlanta, 1987.

[7] P.Pillay and R.Krishnan, “Modelling, Simulation and Analysis of a Permanent Magnet

Brushless DC motor drive part II: The brushless DC motor drive,” IEEE Transactions on

Industry application, Vol.25, May/Apr 1989.

[8] B.K. Bose. Modern Power Electrics and AC Drives. Prentice-Hall, Inc., 2002.

[9] E. Hendawi, F. Khater, and A. Shaltout, “Analysis, Simulation and Implementation of Space Vector Pulse Width Modulation Inverter,” International Conference on Application of Electrical Engineering, pp. 124-131, 2010.

[10] Sathyan, Anand, Nikola Milivojevic, Young-Joo Lee, Mahesh Krishnamurthy, and Ali Emadi. "An FPGA-based novel digital PWM control scheme for BLDC motor drives." *Industrial Electronics, IEEE Transactions on* 56, no. 8 (2009): 3040-3049.

[11] Åström, K. J., and T. Hägglund. "Revisiting the Ziegler–Nichols step response method for PID control." *Journal of process control* 14, no. 6 (2004): 635-650.

[12] Kumar, K. Vinoth, Prawin Angel Michael, Joseph P. John, and Dr S. Suresh Kumar. "Simulation and comparison of SPWM and SVPWM control for three phase inverter." *ARPN Journal of Engineering and Applied Sciences* 5, no. 7 (2010): 61-74.

[13] Rathnakumar, D., J. LakshmanaPerumal, and T. Srinivasan. "A new software implementation of space vector PWM." In *SoutheastCon, 2005. Proceedings. IEEE*, pp. 131-136. IEEE, 2005.

[14] Won, Chang-hee, Joong-Ho Song, and Ick Choy. "Commutation torque ripple reduction in brushless DC motor drives using a single DC current sensor." In*Power Electronics Specialists Conference, 2002. pesc 02. 2002 IEEE 33rd Annual*, vol. 2, pp. 985-990. IEEE, 2002.

[15] Carlson, Renato, Michel Lajoie-Mazenc, and J. C. D. S. Fagundes. "Analysis of torque ripple due to phase commutation in brushless DC machines." *Industry Applications, IEEE Transactions on* 28, no. 3 (1992): 632-638.

[16] Le-Huy, Hoang, Robert Perret, and Rene Feuillet. "Minimization of torque ripple in brushless dc motor drives." *Industry Applications, IEEE Transactions on* 4 (1986): 748-755.

[17] Luk, P. C. K., and C. K. Lee. "Efficient modelling for a brushless DC motor drive." In *Industrial Electronics, Control and Instrumentation, 1994. IECON'94., 20th International Conference on*, vol. 1, pp. 188-191. IEEE, 1994.

[18] MadhusudhanaRao, G., B. V. SankerRam, B. Smapath Kumar, and K. Vijay Kumar. "Speed control of BLDC motor using DSP." *International Journal of Engineering Science and Technology* 2, no. 3 (2010): 143-147.